

**Bioinspired medical needles
a review of the scientific literature**

Fung-A-Jou, Zola; Bloemberg, Jette; Breedveld, Paul

DOI

[10.1088/1748-3190/acd905](https://doi.org/10.1088/1748-3190/acd905)

Publication date

2023

Document Version

Final published version

Published in

Bioinspiration and Biomimetics

Citation (APA)

Fung-A-Jou, Z., Bloemberg, J., & Breedveld, P. (2023). Bioinspired medical needles: a review of the scientific literature. *Bioinspiration and Biomimetics*, 18(4), Article 041002. <https://doi.org/10.1088/1748-3190/acd905>

Important note

To cite this publication, please use the final published version (if applicable).
Please check the document version above.

Copyright

Other than for strictly personal use, it is not permitted to download, forward or distribute the text or part of it, without the consent of the author(s) and/or copyright holder(s), unless the work is under an open content license such as Creative Commons.

Takedown policy

Please contact us and provide details if you believe this document breaches copyrights.
We will remove access to the work immediately and investigate your claim.

TOPICAL REVIEW • OPEN ACCESS

Bioinspired medical needles: a review of the scientific literature

To cite this article: Zola Fung-A-Jou *et al* 2023 *Bioinspir. Biomim.* **18** 041002

View the [article online](#) for updates and enhancements.

You may also like

- [Research on the Design of Recycling Medical Needle Safety Bayonet-Lock Box](#)
Tong-Tong Lan, Shinn-Dar Wu, Po-Wen Tsai et al.
- [Ovipositor-inspired steerable needle: design and preliminary experimental evaluation](#)
M Scali, T P Pusch, P Breedveld et al.
- [A novel adaptive needle insertion sequencing for robotic, single needle MR-guided high-dose-rate prostate brachytherapy](#)
M Borot de Battisti, B Denis de Senneville, G Hautvast et al.

Bioinspiration & Biomimetics



TOPICAL REVIEW

Bioinspired medical needles: a review of the scientific literature

OPEN ACCESS

RECEIVED
21 February 2023

REVISED
25 April 2023

ACCEPTED FOR PUBLICATION
25 May 2023

PUBLISHED
16 June 2023

Original Content from
this work may be used
under the terms of the
[Creative Commons
Attribution 4.0 licence](#).

Any further distribution
of this work must
maintain attribution to
the author(s) and the title
of the work, journal
citation and DOI.



Zola Fung-A-Jou , Jette Bloemberg*  and Paul Breedveld

Bio-Inspired Technology (BITE) Group, Department of BioMechanical Engineering, Faculty of Mechanical, Maritime and Materials Engineering, Delft University of Technology, Delft, The Netherlands

* Author to whom any correspondence should be addressed.

E-mail: j.bloemberg@tudelft.nl

Keywords: bio-inspiration, needle, medical, non invasive surgery, percutaneous, review, instrument

Abstract

Needles are commonly used in medical procedures. However, current needle designs have some disadvantages. Therefore, a new generation of hypodermic needles and microneedle patches drawing inspiration from mechanisms found in nature (i.e. bioinspiration) is being developed. In this systematic review, 80 articles were retrieved from Scopus, Web of Science, and PubMed and classified based on the strategies for needle-tissue interaction and propulsion of the needle. The needle-tissue interaction was modified to reduce grip for smooth needle insertion or enlarge grip to resist needle retraction. The reduction of grip can be achieved passively through form modification and actively through translation and rotation of the needle. To enlarge grip, interlocking with the tissue, sucking the tissue, and adhering to the tissue were identified as strategies. Needle propelling was modified to ensure stable needle insertion, either through external (i.e. applied to the prepuncturing movement of the needle) or internal (i.e. applied to the postpuncturing movement of the needle) strategies. External strategies include free-hand and guided needle insertion, while friction manipulation of the tissue was found to be an internal strategy. Most needles appear to be using friction reduction strategies and are inserted using a free-hand technique. Furthermore, most needle designs were inspired by insects, specifically parasitoid wasps, honeybees, and mosquitoes. The presented overview and description of the different bioinspired interaction and propulsion strategies provide insight into the current state of bioinspired needles and offer opportunities for medical instrument designers to create a new generation of bioinspired needles.

1. Introduction

1.1. Background information

1.1.1. Bioinspired medical needles

Although needles are considered minimally invasive surgical instruments, current needle designs have numerous disadvantages [1]. Two types of needles can be distinguished: hypodermic needles and microneedle (MN) patches. Hypodermic needles are hollow, single needle systems that puncture the skin to inject or subtract matter [2]. The definition of MN patches varies in the literature, but here they are defined as patches with an array of short (length <3 mm) MNs that penetrate the skin, no further than the dermis or epidermis. Hypodermic needles are subject to needle displacement due to needle deformation, organ movement, and human error tissue displacement [3]. This can be problematic for the surgeon in terms of accurately reaching a target, but

it can also cause tissue damage resulting in pain and fear for the patient [4]. In the brain, it can lead to serious consequences such as swelling and bleeding [5]. MN patches are less invasive than hypodermic needles due to their shallow penetration depth and small diameter. However, they still have their disadvantages, such as poor adhesion ability and antimicrobial activity [6], inconsistent drug distribution, durability issues [7], and strength issues. MNs are prone to bending or breaking during manual insertion or having high deviations in insertion height when inserted into soft and inhomogeneous skin tissue [8].

The proposed solutions for improving needles by, for instance, making them sharper and thinner are limited [4]. Therefore, a new generation of needles that draws inspiration from mechanisms found in nature, such as stingers, thorns, teeth, tongues, or quills, is being developed. This approach is called bioinspiration, which is the art of studying nature

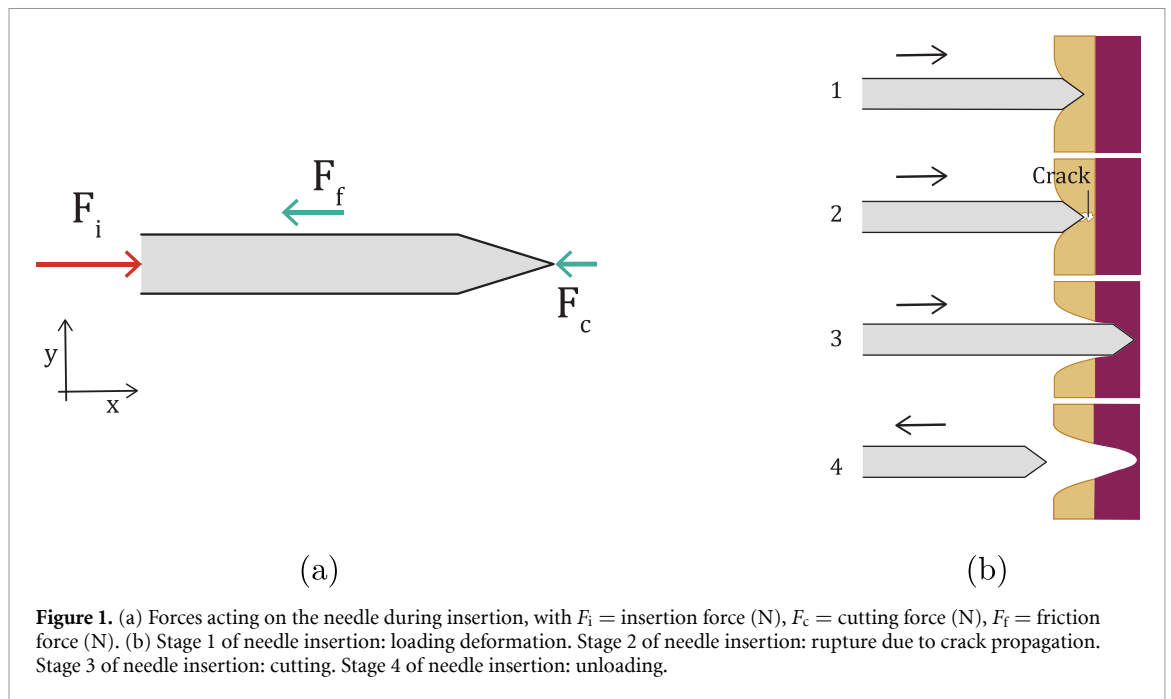


Figure 1. (a) Forces acting on the needle during insertion, with F_i = insertion force (N), F_c = cutting force (N), F_f = friction force (N). (b) Stage 1 of needle insertion: loading deformation. Stage 2 of needle insertion: rupture due to crack propagation. Stage 3 of needle insertion: cutting. Stage 4 of needle insertion: unloading.

and its principles and exploring ways to implement those principles and mechanisms into novel solutions. While there is still much to discover about their design and manufacturability, bioinspired needles have the potential to revolutionize medical healthcare. They can be used for a variety of percutaneous procedures (i.e. medical procedures through the skin), including drug delivery, blood extraction, focal therapy, and biopsies. Throughout this article, the term ‘needle’ refers to the bioinspired medical needle, while the term ‘stinger’ refers to the animal stinger.

1.1.2. Needle mechanics

Different forces come into play when a needle punctures the skin and moves through the tissue. The forces acting on a needle include the cutting force (F_c) and the friction force (F_f) (figure 1(a)). The cutting force acts normal to the bevel surface as a result of cutting the tissue, this includes the plastic deformation acting from the soft tissue and the force resulting from the tissue stiffness at the tip. The friction force (F_f) acts along the needle shaft due to friction between the needle and tissue and is also a function of the internal stiffness of the soft tissue. Due to bending of the needle, there exist x - and y -components of the forces, with the x -components being counteracted by the insertion force (F_i), which is the force required to insert the needle into the tissue. The insertion force is defined as [9]:

$$F_i = F_{f,x} + F_{c,x} \quad (1)$$

The insertion force can be decreased by decreasing the friction force and/or the cutting force. The friction force might be changed using the relative velocity or the contact area [9]. Decreasing the cutting force

causes a decrease of the tissue damage which results in less pain and a faster recovery.

Figure 1(b) shows the needle insertion process divided into the following four stages where different forces play a role [10]:

1. Loading deformation: the needle advances outside the tissue and pushes against the skin, while the needle insertion force increases;
2. Rupture: a crack propagates into the tissue at the maximum insertion force and the insertion force drops;
3. Cutting: cutting event after rupture, where the crack gets larger in line with the needle displacement;
4. Unloading deformation: needle insertion stops and needle is removed.

During stages 1 and 2 (i.e. puncturing), the cutting force plays a more significant role, whereas during stages 3 and 4 (i.e. internal insertion), the friction force is more important. In the case of MN patches, the puncturing of the skin (stages 1 and 2) is more significant than the internal movement through the tissue, since the MNs do not go deeper than the skin layers, whereas for hypodermic needles, the movement through the tissue (stages 3 and 4) and bending of the needle are more significant than the puncturing of the skin, since the needles travel a longer distance through the tissue.

1.2. Problem definition

In the relatively new field of using bioinspiration in medical instrument design, designers may feel overwhelmed in the vast amount of bioinspiration sources and potential strategies. This study focuses on the scientific literature to provide guidance on

the bioinspiration sources, medical applications, and manufacturing methods of the proposed needle designs. Although some reviews on bioinspired MN patches [11] and mosquito-inspired needles [12] exist, to our knowledge, no comprehensive overview of all bioinspired needles in the scientific literature is available.

1.3. Goal and structure

This study presents an overview of the scientific literature on bioinspired medical needles. An overview of the scientific literature on bioinspired medical needles provides insights into the future development and direction in the field of bioinspired needles and identifies opportunities for innovation. In section 2, the method used to collect all included articles is described. Sections 3 and 4 outline the classification of the collected articles. Finally, the findings and future perspectives are discussed in section 5.

2. Method

2.1. Literature search

To create a comprehensive overview of the current developments of bioinspired needles, a search in Scopus, Web of Science (WoS), and PubMed was performed (last update: 31 January 2023). This search was executed systematically by dividing the research goal into two related concepts: ‘Device’ and ‘Approach,’ and search terms were generated for each concept (table 1). The field (e.g. medical) and function (e.g. surgery) were excluded as search concepts, as including them would have led to a limited selection of articles. For Concept 1, the search term ‘*Needle*’ was the only term used because other equivalents such as ‘probe’ or ‘medical instrument’ were found to be too general and did not generate more relevant articles. For Concept 2, commonly used synonyms of bioinspiration found in the literature were included. The term ‘biomechanical’ was excluded, since the results showed mechanical models of biological principles instead of bioinspired designs. The search query was limited to articles written in English, and conference articles were excluded because they were already covered in the regular search. The search was executed in the title, abstract, and keywords of Scopus, the topic operator (TS) of WoS, and the title and abstract of PubMed. The resulting Scopus query, adjusted for WoS and PubMed (appendix A), was as follows: *TITLE-ABS-KEY ((bio-inspir* OR bioinspir* OR “Biolog* inspire*” OR biomim* OR “Nature inspir*” OR Nature-inspir* OR bionic*) AND (*needle*)) AND (LIMIT-TO (LANGUAGE, “English”)) AND (EXCLUDE (DOCTYPE, “cr”))*.

2.2. Eligibility criteria

The following criteria were used to select articles from the search results. An article was included if it featured

Table 1. Concepts and corresponding search terms.

| Concepts: combine with AND | | |
|----------------------------|--------------------------|----------------------------|
| Search terms: | Concept 1: Device | Concept 2: Approach |
| combine with | *Needle* | Bioinspir* |
| OR | | Bio-inspir* |
| | | “Biolog* inspi*” |
| | | Biomim* |
| | | “Nature inspir*” |
| | | Nature-inspir* |
| | | Bionic* |

a bioinspired needle design that was either tested in the physical world or through computational modeling, where ‘bioinspired’ was defined as incorporating aspects of a mechanism found in nature. The term ‘needle’ was defined as a slender hollow instrument used for introducing matter or removing matter from the body (as by insertion into the skin), or an extremely thin solid instrument used for acupuncture and inserted through the skin [13].

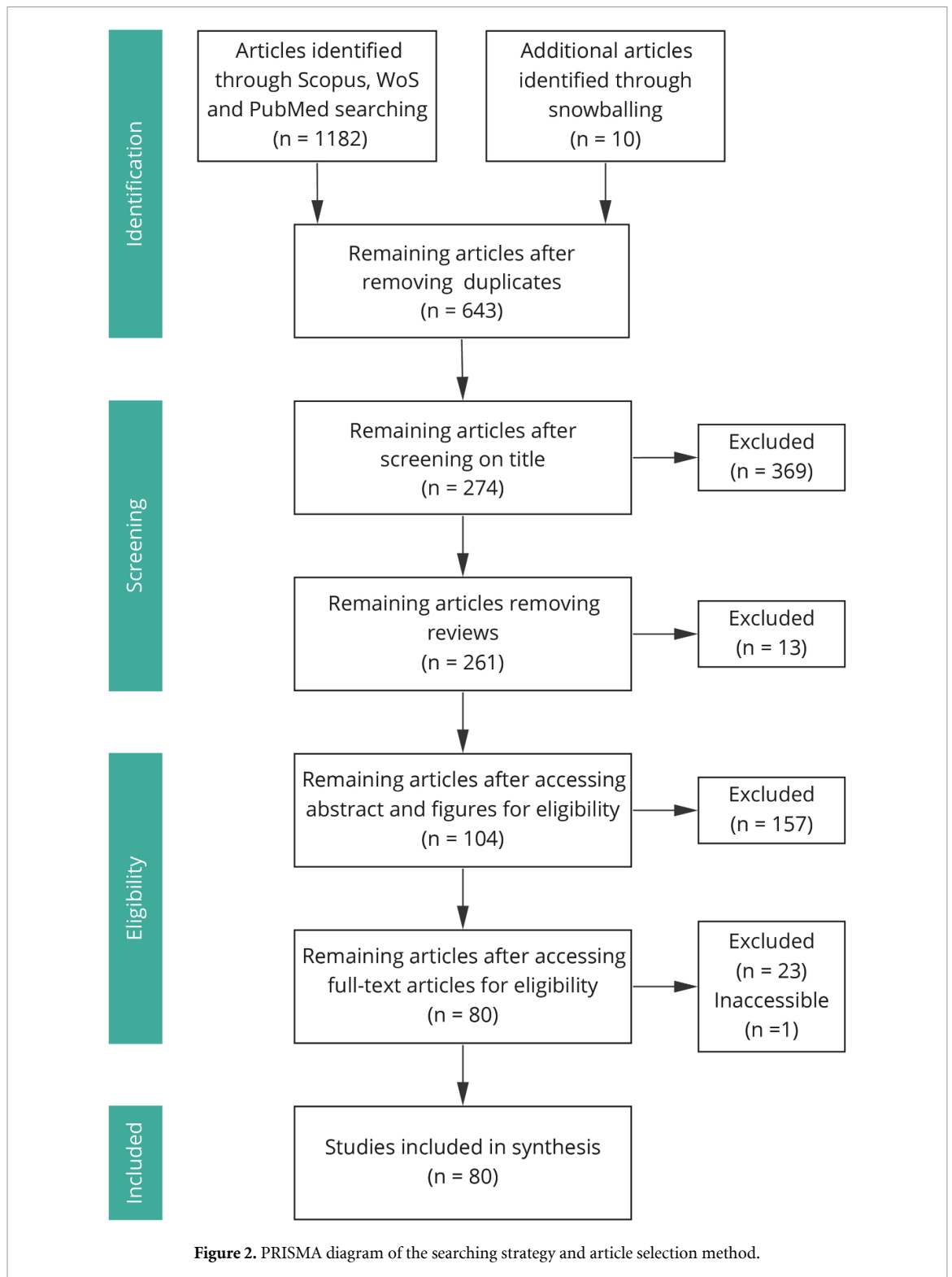
Because we focused specifically on needle designs, we excluded scaffolds with a nanoneedle-shaped bioinspired structure, as well as needle-like hydrophobic surfaces, bioinspired phantoms or materials (e.g. tea extract or hair), robot-needle systems, and control systems, where a description of the needle was not provided. Additionally, we excluded instances of misuse of the term ‘bioinspired,’ where the source of bioinspiration was not named, and it was unclear which aspects were used in the design. Finally, we excluded general bioinspired coatings or multifunctional hydrogels that were not specifically designed for a needle.

2.3. Literature search results

The search resulted in 555 articles in Scopus, 485 articles in WoS, and 143 articles in PubMed. After removing duplicates, a total of 633 unique articles remained. The references of the reviews found in these 633 articles were scanned (snowballing), resulting in the inclusion of an additional ten articles, bringing the total to 643 articles. The titles of these articles were screened, leaving 274 articles. In addition, 13 reviews were excluded since these would contain articles that were already included in this review. The remaining articles were evaluated based on their abstract and figures using the criteria outlined in section 2.2, resulting in the exclusion of 157 articles. Upon full-text reading, 24 articles were excluded for not meeting the eligibility criteria, resulting in the inclusion of 80 articles in this review (appendix B). Figure 2 shows an overview of the search results.

2.4. Classification

The collected articles were classified into two categories, namely ‘interacting’ and ‘propelling,’ as presented in figure 3. ‘Interacting’ refers to the



interaction between the needle and tissue, which can be altered to reduce or enlarge grip, as explained in sections 3.1 and 3.2. ‘Reducing grip’ was further subdivided into two types of needles: needles that passively reduce grip (e.g. by adjusting the form of the needle using barbs) and needles that actively reduce grip (e.g. by applying a rotating or translating motion during needle insertion). ‘Enlarging grip’ was divided into three types of needles that use interlocking (e.g.

using thorns), sucking (e.g. using suction cups), and adhering (e.g. using an adhesive layer) strategies. As for ‘propelling,’ it was classified into the needle’s prepuncturing movement outside the body (i.e. external) and postpuncturing movement through the body (i.e. internal), of which the different strategies are discussed in section 4. ‘External’ was classified into free-hand needle insertion and guided needle insertion.

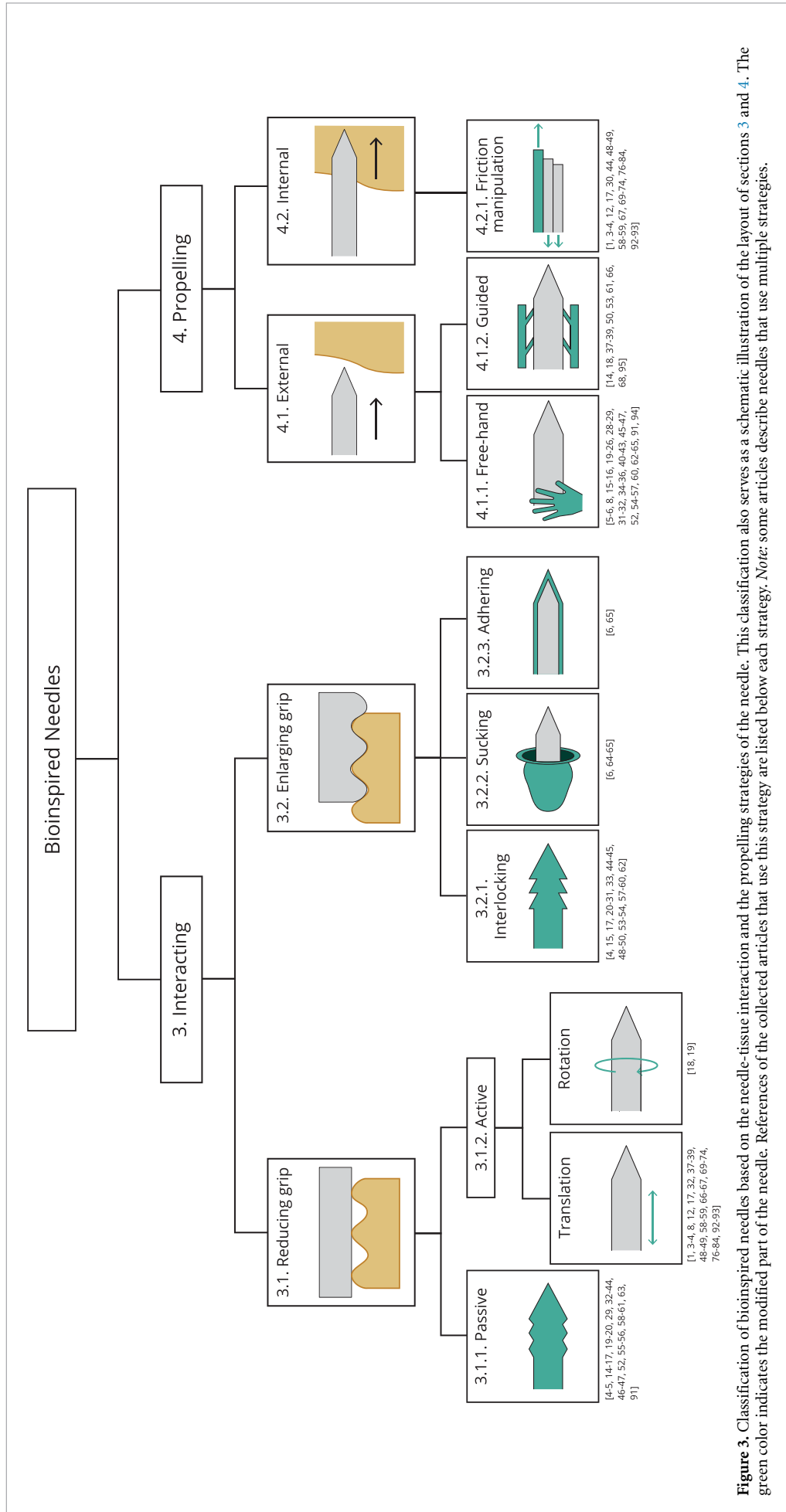


Figure 3. Classification of bioinspired needles based on the needle-tissue interaction and the propelling strategies of the needle. This classification also serves as a schematic illustration of the layout of sections 3 and 4. The green color indicates the modified part of the needle. *Note:* some articles describe needles that use multiple strategies.

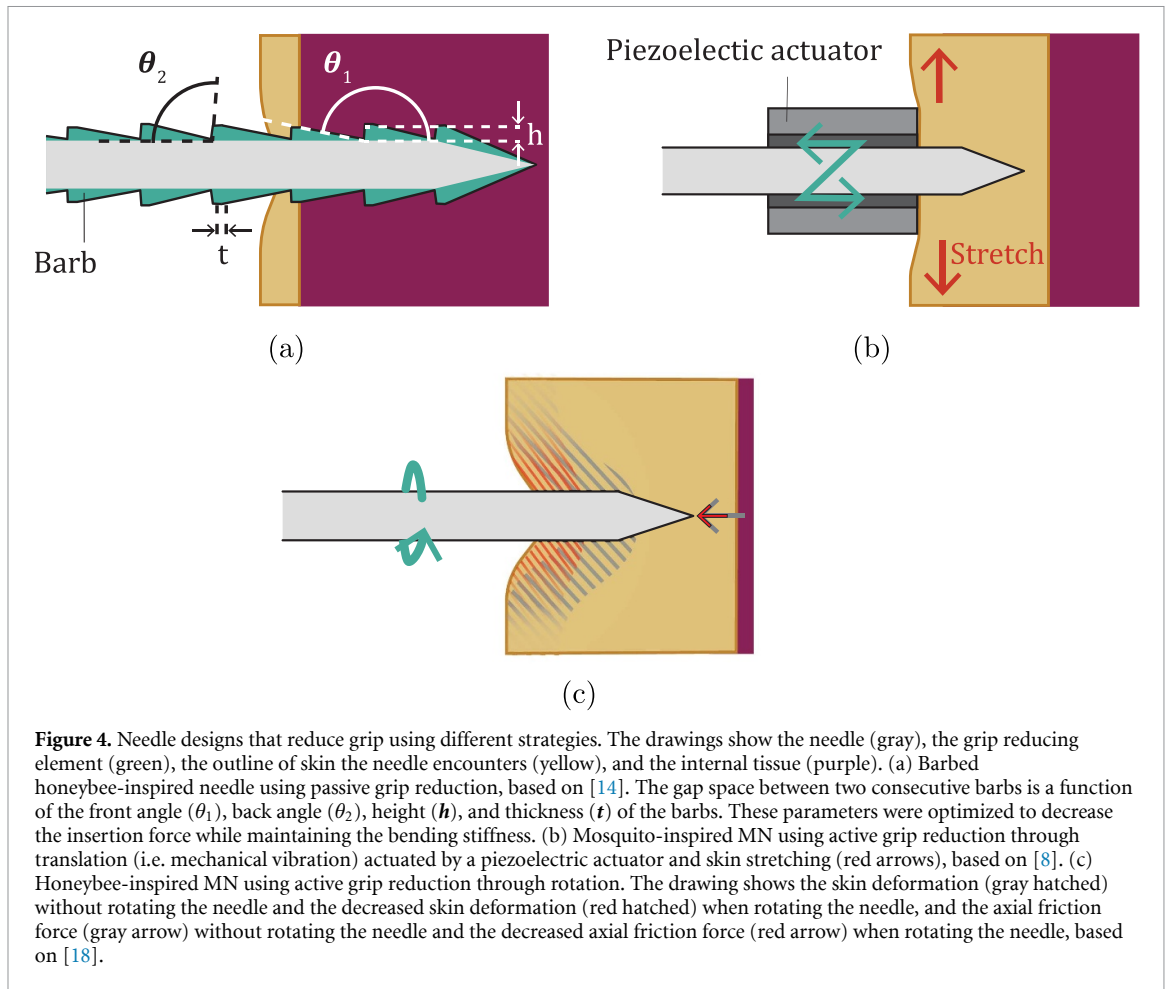


Figure 4. Needle designs that reduce grip using different strategies. The drawings show the needle (gray), the grip reducing element (green), the outline of skin the needle encounters (yellow), and the internal tissue (purple). (a) Barbed honeybee-inspired needle using passive grip reduction, based on [14]. The gap space between two consecutive barbs is a function of the front angle (θ_1), back angle (θ_2), height (h), and thickness (t) of the barbs. These parameters were optimized to decrease the insertion force while maintaining the bending stiffness. (b) Mosquito-inspired MN using active grip reduction through translation (i.e. mechanical vibration) actuated by a piezoelectric actuator and skin stretching (red arrows), based on [8]. (c) Honeybee-inspired MN using active grip reduction through rotation. The drawing shows the skin deformation (gray hatched) without rotating the needle and the decreased skin deformation (red hatched) when rotating the needle, and the axial friction force (gray arrow) without rotating the needle and the decreased axial friction force (red arrow) when rotating the needle, based on [18].

3. Interacting

3.1. Reducing grip

Two-thirds of the collected articles present needle designs that aim to reduce the grip between the needle and tissue. Figure 3 shows passive and active strategies for grip reduction, such as adjusting the form of the needle, translating (i.e. vibrating), or rotating it. Often, multiple strategies are combined to optimize grip reduction.

3.1.1. Passive

Thirty-three articles were collected presenting needles that use passive grip reduction through form modification. This strategy was the most commonly used strategy for grip reduction. It is also found in nature where it occurs in a large variety of organisms, such as insect stingers, thorns of plants, and even natural phenomena like ice formation. The mosquito and honeybee are most commonly used as sources of bioinspiration, as both have barbs on their stinger to distribute the insertion forces between the stinger and tissue. This strategy can be applied to both hypodermic needles and MN patches. Most designs did not specify a medical application and were designed for percutaneous procedures.

Sahlbadi and Hutapea [14] developed a needle for percutaneous procedures such as brachytherapy, brain surgery, and biopsy, mimicking the barbs of a honeybee stinger (figure 4(a)). The design was optimized to decrease the insertion force resulting in a decrease in tissue damage and pain and a higher targeting accuracy. The three-dimensional (3D)-printed polymer needle has a diameter of 1–3 mm and a length of 180 mm, with barbs revolved around the needle axis. The barbs form gaps on the needle surface, resulting in a smaller frictional area and thus reducing the insertion force. The gap space between two consecutive barbs is a function of the front angle, back angle, height, and thickness of the barbs, which were optimized to decrease the insertion force while maintaining the bending stiffness. The design led to a total reduction in insertion force of 35% in polyvinyl chloride (PVC) gel and 46% in liver tissue compared to conventional needles with a point or bevel tip. Experiments showed a decrease of 21%–26% in the insertion force regardless of the needle scale.

Notably, all long hypodermic needles (i.e. needle length >60 mm) were inspired by various insect stingers, such as those of the honeybee, parasitoid wasp, and mosquito. Needles developed for blood extraction were all inspired by the mosquito. The inspiration for smaller hypodermic needles and MN

patches is much more diverse, with plants [15], mammals, birds, reptiles, and even a natural phenomenon based on the formation of ice [16] used as sources of inspiration for minimizing the insertion forces through form modification (i.e. passive grip reduction).

3.1.2. Active

3.1.2.1. Translation

Thirty-three articles were collected presenting needles that use translation as a strategy for grip reduction. In nature, this strategy is found in bees, wasps, and mosquitoes that can alter the vibration frequency of their stingers. The parasitoid wasp was the most commonly used source of inspiration for friction manipulation, which enables self-propelling properties, section 4 elaborates on this topic. The remaining 11 articles were all inspired by the mosquito and contained designs for hypodermic needles and MN patches. The most frequently described medical application was blood extraction, which matches the blood-sucking function of the female mosquito proboscis (i.e. mouthpart for feeding and sucking).

Kim *et al* [8] investigated the effect of mechanical stimuli on insertion forces as background information for a drug delivery MN patch inspired by the mosquito proboscis (figure 4(b)). The mosquito proboscis consists of a labrum, a hollow needle in the center with capillary capacities for blood-sucking, and two maxillae placed to the left and right of the labrum with a jagged shape for anchoring the tissue, surrounded by a labium. Mosquitoes use two distinct motions while piercing the skin: (1) pressing down their labium to stretch the skin and (2) vibrating their fascicle bundle; both motions change the skin resistance. These static and dynamic mechanical stimuli were tested *ex vivo* with standard cylindrical stainless steel acupuncture needles with a diameter of 60–140 μm and an insertion velocity of 0.1–2 mm s^{-1} on porcine skin. To test the static stimulus, the skin was stretched 0%–20%, and it was found that this mainly affects the insertion precision. To test the dynamic stimulus, the needle was vibrated with a frequency of 1–1000 Hz and amplitude of 1–10 μm , and the authors concluded that it controlled the degree and deviation of skin resistance. The result was a deep, easy, and controlled insertion with low insertion forces.

Suzuki *et al* [17] designed a hypodermic MN for painless blood extraction, using the same properties as the female mosquito proboscis. The needle was composed of two half-needles with a semicircular channel and jagged edges combined into a hollow needle, with capillary force for blood extraction. The jagged edges have interlocking features that are discussed in section 3.2.1. The total needle has a length of 2 mm and diameter of 0.1 mm, and it moves forward by advancing the labrum and maxillae

alternately. The needle was fabricated with an ultra-precision 3D laser lithography system, based on the two-photon absorption phenomenon. Photocurable polymer materials IP-Dip and IP-S were cross-linked with a laser beam, positioned by a computer-aided design model. The needle was tested in artificial skin and it was found that vibration motion is effective for reducing the insertion force. The insertion force was also reduced for an alternately advanced motion. However, the difference between no vibration, alternating vibration, and in-phase vibration was not clearly distinctive.

3.1.2.2. Rotation

Two articles were collected presenting needles that use rotation as a grip reduction strategy. In nature, this strategy is employed by honeybees with a rotating stinger shaft and flies (*Stomoxys*) with rotating teeth for tearing open tissue [18]. Rotation was demonstrated in both hypodermic needles and MN patches for percutaneous procedures, drug delivery, or biomarker monitoring. It was used as an alternative to ‘passive grip reduction’ to maintain the mechanical robustness of the needle and save manufacturing costs.

Cai *et al* [18] employed this strategy to design a biomonitoring MN patch based on the honeybee’s rotating stinger (figure 4(c)). The objective was to achieve higher needle strength and lower deviation in insertion depth than conventional MN patches. A commercial stainless steel acupuncture needle was used as substitute for a MN with a conical tip, a diameter of 0.21 mm, and a length of 1.2 mm. The design aimed to reduce the internal insertion force, i.e. the insertion force after puncturing the skin, by decreasing the friction force, which has the highest contribution to the insertion force. Finite element method tests and *ex vivo* porcine skin tests showed a 45.7% reduction in the maximum insertion force. The authors also showed that the insertion force decreased by increasing the rotational velocity, up to a certain point. Furthermore, there was a decrease in skin deformation and a faster skin recovery while holding the needle inside the skin.

Wang and Cong [19] developed a needle that was not designed for rotation, but rotation occurred as a favorable side effect. The hole pattern of the mole cricket’s tergum and the Chinese sturgeon’s skin were mimicked to create an injection needle that could reduce pain without limiting the insertion depth. A syringe needle with a diameter of 1.6 mm and a length of 25.4 mm was modified using machining to create a pattern of holes along the needle shaft. The holes reduced the contact area between the needle and skin tissue, resulting in a reduction of friction as the needle moved through the skin tissue. Furthermore, due to the holes, the needle wall, air, and skin tissue formed a rolling bearing model that contributed to the drag reduction. Simultaneously, micro-vibrations arose in

the skin tissue, which increased both the flow speed of the biological fluids and the lubrication effects. The needle surface design with a hole diameter of 0.09 mm and a hole interval of 0.9 mm resulted in a 44.05% drag reduction in silicon compared to smooth syringe needles.

In the collected articles, the needle designs that employed active strategies are less divers than those utilizing passive strategies. The bioinspiration was mainly drawn from the mosquito, parasitoid wasp, honeybee, and mole cricket, and only a small number of articles described needles that apply these strategies.

3.2. Enlarging grip

Enlarging grip might be necessary for stable drug delivery in MN patches and stable needle insertion of hypodermic needles. Three strategies can be employed for this: (1) mechanical interlocking, (2) sucking, and (3) adhering.

3.2.1. Interlocking

Twenty-eight articles were collected presenting needles that use interlocking as a strategy to enlarge grip, where three different methods can be distinguished. The first method is using the same passive strategy to reduce grip, but now modifying the form in order to enlarge grip. This is seen in nature in the porcupine and wasp that have barbs on their quills and stinger, respectively, to anchor to their predator's skin as a form of self-defense [20, 21]. Moreover, it is seen in thorns of plants and many parasites to anchor to their host. The second method is clamping, which is seen in the claws of eagles and mantises, as well as the mouths of lampreys and sharks [22–25]. The third method is swelling, used by endoparasites to anchor themselves to their host's intestinal walls [26, 27]. Mechanical interlocking was only applied in MN patches and short hypodermic needles that do not go deeper than the epidermis. It is most commonly used for medical applications like drug delivery and blood extraction.

Some needles that were designed for interlocking strategies had the positive side effect of also lowering the puncture force as described in section 3.1.1, resulting in a low insertion force and high tissue adhesion [20]. To illustrate, Liu *et al* [28] designed a MN for prolonged monitoring and drug release in the intestines based on the proboscis of the parasitic spiny-headed worm (figure 5(a)), which has barbs along its proboscis to move through the gut with minimal locomotion. Scanning electron microscopic (SEM) images of the proboscis were converted to a hollow needle design with a diameter of 108–74 μm from base to tip and a length of 1 mm. This length is necessary for puncturing the gut wall and reaching the mucus blanket and epithelial barrier. The barbs, with a diameter, length, and curve of respectively 8 μm , 40–30 μm , and 50°, are equally distributed over a

length of 0.5 mm from the needle tip, which is the most effective barb region. The MNs were 3D-printed with direct laser writing, which uses two-photon photopolymerisation to cure photoresist, and were then attached to a polydimethylsiloxane (PDMS) backing. This technique has high precision and is suitable for manufacturing the overhanging barbs. The barbed needle design showed a significant increase of the retraction force compared to barbless needles while maintaining a low insertion force, when tested in *ex vivo* porcine small-intestine tissue. Compared to other state-of-art barbed MNs (e.g. the honeybee-inspired needle [29]), the retraction force remained the same while the insertion force is two times smaller resulting in a ten times higher retraction/insertion force ratio.

Zhang *et al* [23] used inspiration from the serrated microstructure of the mantis' forelegs to design a minimally invasive drug delivery MN patch (figure 5(b)). Using SEM imaging, the forelegs of the mantis were observed and converted to a ferrofluid-configured mould. This mould was filled with a biocompatible polymer for transdermal drug delivery (TDD) (i.e. 50 ml of silk fibrion solution 30% w/v) and cured under ultraviolet (UV) light. The resulting MN patch consists of MNs with different diameters and lengths around 0.25 μm and 0.6 μm , respectively, and with an inclination angle ranging from 30° to 90°. Because of this inclination angle, the MN patch has the same grasping and holding properties as the mantis and clamps itself to the tissue. A rotation-and-load-bearing test was performed on *ex vivo* porcine skin and showed a decrease in the inclination angle of the MNs enhanced the ability of the MN patch to withstand external forces. An angle of 30° showed the best holding capabilities, while the patch with 90°-MN inclination angles (i.e. perpendicular to the surface) would immediately fall off. This result was confirmed by a second test where the MN patches were attached to living mice. These second tests also showed successful insertion of the MNs and rapid recovery of the tissue. Lastly, the *in vivo* mice tests and *in vitro* tests showed a sustained drug delivery.

Another way of interlocking was applied by Jeon *et al* [26] and Yang *et al* [27] who designed swellable MN patches based on the swelling properties of endoparasites (figure 5(c)). Yang *et al* [27] used inspiration from the spiny-headed worm, specifically the *Pomphorhuncus Laevis*, for a drug-delivery MN patch. The spiny-headed worm uses its proboscis to puncture the intestinal wall of its host, where it expands a bulb using its retractor muscles at the base of its proboscis to interlock the proboscis and the intestinal wall tissue. The MN patch was designed applying a similar method to interlock the MN patch and the tissue. The cone-shaped MNs with a base diameter of 280 μm and a length of 700 μm have a hydrophobic non-swellable core and a hydrophilic swellable outer layer. The hydrophilic outer layer absorbs the

tissue fluids and swells to 20% of the tip height into a mushroom shape, while the core remains stiff. The MN patch was fabricated in a PDMS mould, filled with a polystyrene (PS)-block-poly(acrylic acid) casting (i.e. outer layer) and PS homopolymer filling (i.e. core). Tests in hydrogel showed that it takes 10 min for the MNs to get into the maximum swollen state and 15 min to recover back to its conical shape after removal. It also showed that the MN patch could be removed without breaking it and that the adhesion strength significantly increased when the MNs were in their swollen state. Multiple movement cycles with pig joints were executed to show that a strong fixation was achieved. Tests in intestine mucosal tissue showed a 3.5 times increase of adhesion strength compared to staples and a removal force of 4.5 N cm^{-2} . The results were minimal tissue damage, reduced infection risk, and a sustained delivery of bioactive therapeutics.

Twelve articles were collected presenting needles that use both 'passive grip reduction' and 'interlocking for grip enlargement' strategies. In these needle designs, the form of the needle was modified for smooth insertion, and interlocking mechanisms were applied to resist retraction. Table 2 displays various needle tips that use form modification for grip enlargement and/or grip reduction, demonstrating the numerous possibilities of bioinspiration for the same strategy, while applying different implementation methods. Again, all blood-extraction needles are based on the mosquito's proboscis, and the designs adopted different properties of proboscis, such as vibration or form modification [4, 30]. Interestingly, the swellable needle developed by Yang *et al* [27] swells to form a mushroom shape, while Li *et al* [31] uses a stiff mushroom shape as the favourable geometry for interlocking tissue.

3.2.2. Sucking

Three articles were collected presenting needles that use sucking as a strategy to enhance grip, with two of the three designs using it in combination with adhering. All needles use bioinspiration from the octopus and the suction cups on its tentacles. This suction strategy was found solely in MN patches with drug delivery as the medical application.

The single article presenting a needle that used only suction as a strategy to enhance grip was published by Fu *et al* [64], who designed an MN patch for pancreatic cancer treatment inspired by the suction cups on the tentacle of the octopus. The MN patch consists of an array of MNs with suction cups in between, which can adhere to the irregular surface of tumors. The MNs have a conical shape with an estimated diameter of $450 \mu\text{m}$ and a length of $600 \mu\text{m}$. The suction cups have a conical cavity and mimic the octopus tentacle. The whole MN patch was made of a gelatin methacryloyl (GelMA) hydrogel that was poured in a mould and cured with UV light. A peeling-strength test on *ex vivo* porcine pancreas






























demonstrated that the suction cup MN patch adhered better than a conventional MN patch. The capacity for drug delivery was measured, and it was confirmed that the drug release kinetics could be mediated by adjusting the concentration of GelMA hydrogel. The MN patch was tested *in vivo* on mice with tumors, alongside a conventional treatment method, and a control group. The results showed no difference between the intraperitoneal injection and the suction cup MN patch, indicating good tolerability, biocompatibility, and biosafety. It demonstrates that the suction MN patch could induce pancreatic cancer cell apoptosis by releasing the carried gemcitabine.

Joymungul *et al* [65] proposed a gripe-needle design based on both the sucking and adhering capabilities of the octopus' suction cup to perform an incision task in the optic nerve area (figure 5(d)). The gripe-needle was based on the octopus' technique for grasping and boring sea snail shells. The stickiness of the octopus' suction cup increases sealing and surface contact with the shell, while the suction chamber creates a pressure gradient to maximize force grip. Once the shell is in a stable position, the octopus drills a hole into it with its radula (i.e. mouthpart). The gripe-needle consists of a cone-shaped suction cup made using photopolymer resin 3D printing with double-sided adhesive acrylic gel tape with cut grooves attached to its base. A nitinol outer tube connects the top of the cup to a Y-junction (i.e. the suction chamber), which is made of two rubber caps of 7 mm and 12 mm in diameter, respectively. A suction syringe is connected to the air-tight Y-junction to create an under pressure. A drug-delivery syringe is attached to another nitinol tube that can move coaxially inside the outer tube. Four variations of the prototype were made to test the feasibility of the design in four experiments, respectively: (1) a proof-of-concept prototype showed sufficient gripping and shear force on different materials in wet and dry conditions, (2) a test on bubble wrap showed successful incision, (3) an eye-sample test showed successful access to the optic nerve, and (4) tests on a porcine eye sample showed a force grip above the required 1 N, however, this force was not maintained effectively during insertion. Overall, the gripping force significantly increases on semi-rough surfaces when increasing the suction cup pressure. During the incision task, the grooves maintained vacuum grip and increased cup adhesion, but decreased the cup's lifetime. Pulling and shear loading tests showed that the surface wetness enhanced vacuum grip.

3.2.3. Adhering

Zhang *et al* [6] used a combination of suction and adhesion strategies inspired by the octopus and mussel in the design of a multifunctional MN patch for drug delivering (figure 5(e)). In addition, the authors incorporated antibacterial properties based on the *Paenibacillus polymyxa* bacteria that restrain

Table 2. Needle tip designs that use form modification to reduce grip during tissue insertion and/or mechanical interlocking to enlarge grip during retraction. Illustration of the source(s) of bioinspiration, source(s) of bioinspiration, medical application(s), ability to reduce grip for smooth needle insertion (yes or no), ability to increase grip to resist needle retraction (yes or no), and reference(s).







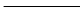
| Illustration | Bioinspiration | Medical application | Reduce grip for smooth insertion | Increase grip to resist retraction | References |
|---|-------------------------------|-------------------------------------|----------------------------------|------------------------------------|-----------------|
|  | Mosquito | Percutaneous procedure | yes | no | [32] |
|  | Honeybee | Percutaneous procedure | yes | yes | [29, 33] |
|  | Porcupine | Percutaneous procedure | yes | yes | [20] |
|  | Lamprey | Wound healing | no | yes | [22] |
|  | Parasitoid wasp | Percutaneous procedure | yes | no | [34–36] |
|  | Mosquito | Percutaneous procedure | yes | no | [37, 38] |
|  | Mosquito, Honeybee | Biopsy, Percutaneous procedure | yes | no | [5, 14, 39–41] |
|  | Mosquito | Biopsy | yes | no | [42] |
|  | Snake | Drug delivery | yes | no | [43] |
|  | Mosquito | Drug delivery | yes | yes | [44] |
|  | Shark | Wound healing | no | yes | [25] |
|  | Mosquito, Honeybee, Porcupine | Drug delivery | no | yes | [45] |
|  | Mosquito | Blood extraction | yes | no | [46] |
|  | Mosquito | Blood extraction | yes | no | [47] |
|  | Mosquito | Blood extraction | no | yes | [30, 48, 49] |
|  | Mosquito | Biopsy | no | yes | [50] |
|  | Mosquito | Deep brain simulation | yes | no | [51] |
|  | Mushroom | Drug delivery, Information storage | no | yes | [31] |
|  | Limpet | Drug delivery | yes | no | [52] |
|  | Golden margined century plant | Performance monitoring | yes | yes | [15] |
|  | Spiny-headed worm | Drug delivery, Biomarker monitoring | no | yes | [53] |
|  | Spiny-headed worm | Drug delivery, Biomarker monitoring | no | yes | [53] |
|  | Honeybee | Myocardial infarction treatment | no | yes | [54] |
|  | Bird bill | Drug delivery | yes | no | [55] |
|  | Mosquito | Blood extraction | yes | no | [56] |
|  | European true bug | Drug delivery | no | yes | [57] |
|  | Mosquito | Blood extraction | yes | yes | [4, 17, 58, 59] |
|  | Honeybee | Percutaneous procedure | yes | yes | [60] |
| no image | Mosquito | Blood extraction | yes | no | [61] |
|  | Kingfisher, Porcupine | Wound healing | no | yes | [62] |

(Continued.)

the growth of other bacteria. The MN patch consists of a flexible polydopamine (PDA) hydrogel base, which is equipped with an array of poly(ethylene glycol) diacrylate (PEGDA)-sodium alginate MNs that have a diameter of 300 μm and length of 600 μm . Each MN is encircled by six concave chambers with a diameter of 375 μm and a dome-like protuberance inside, integrated into the base. The MN patch was

produced using a mould in which the material was cured. To replicate the molecular structure of the mussel's protein, a part of the dopamine in a mixture with gelatin was oxidized and cross-linked to the gelatin through chemical reactions. The oxidized and unoxidized dopamines formed a stable PDA hydrogel through various interactions, of which the various inner chemical groups enabled adhesion. The PDA

Table 2. (Continued.)

| Illustration | Bioinspiration | Medical application | Reduce grip for smooth insertion | Increase grip to resist retraction | References |
|---|--------------------------------|------------------------|----------------------------------|------------------------------------|------------|
|  | Mole cricket, Chinese sturgeon | Percutaneous procedure | yes | no | [19] |
|  | Mosquito | Percutaneous procedure | yes | no | [63] |
|  | Spiny-headed worm | Drug delivery | no | yes | [27] |
|  | Ladybug, wasp | Wound healing | no | yes | [21] |
|  | Eagle | Wound healing | no | yes | [24] |
|  | Mantis | Drug delivery | no | yes | [23] |
|  | Ice | Drug delivery | yes | no | [16] |

hydrogel also possessed supramolecular interactions, giving the MN patch self-repairing properties. The PDA-hydrogel base mimics the microstructure of the octopus tentacle, giving it sucking abilities in dry, wet, and moist environments. The antimicrobial peptin polymyxin of the *P. polymyxa* bacteria was loaded at both the MN tips and PDA base. The self-repairing properties were tested by putting two MN patch segments together, the segments would immediately weld together without external stimuli. *Ex vivo* porcine skin tests demonstrated that the MN patch strongly adhered to the skin when lifted, bent, and moisturized or immersed in water. A knuckle test was performed, which showed excellent adhesion when bent along the knuckle up to 90°. A weight test showed adhesion up to 60 kg, which is 240 times its own mass. A peeling-off test was conducted to compare the multifunctional MN patch to (1) an MN patch without PDA hydrogel and without suction cups (i.e. a normal MN patch), (2) an MN patch with only a PDA hydrogel base, and (3) an MN patch with only suction cups. The multifunctional MN patch performed best under overall circumstances, while the normal MN patch performed worst. A rat model showed sustained drug release and less inflammation compared to the MN patch without polymyxin. Lastly, the study demonstrated that the polymyxin killed 80% of the *E. coli* bacteria.

4. Propelling

4.1. External

4.1.1. Free-hand

The majority of the collected articles, 40 out of 80, present a needle design that utilized the strategy of free-hand insertion, encompassing all needles that were not designed for propelling. Almost all MN patches, 21 out of 22, were inserted free-hand, as they were only meant to puncture the skin layers and allow the drug to distribute itself without the need to reach a specific target, unlike hypodermic needles, which require a surgeon to ensure accuracy to reach the desired target. This strategy did not employ any

bioinspiration, and due to the large number of articles in this category, a wide range of medical applications were described.

4.1.2. Guided

Eleven articles were collected presenting needles that used guidance as a strategy for safe needle insertion. This strategy is mostly used for hypodermic needles, although Cai *et al* [18] employed guidance for an MN patch. The mosquito was the primary source of inspiration for these designs, although the honeybee and fly were also used.

Suzuki *et al* [66] were inspired by the mosquito and developed a needle-guidance system for stable insertion of needles with a diameter of 100 μm or less for blood extraction, or drug delivery. The needle-guidance system is based on the needle-like proboscis of the mosquito, which has a diameter of 50 μm that is wrapped in its labium and punctures the skin while grasping the proboscis with the tip of its labium. This technique shortens the effective length of the proboscis, preventing buckling. The needle-guidance system consists of a solid stainless steel acupuncture needle, with a diameter of 100 μm and a length of 4 mm. This needle was placed into a compliant mechanism, of which the components were cut out of a polyacetal (POM) 0.5 mm thick plate using femtosecond laser cutting. The components were fixed together with epoxy adhesive and had a polycarbonate cover. The buckling load in soft tissue depends on the needle length, needle end state, needle material, and tissue stiffness and is expressed as [67]:

$$P = n\pi^2 \frac{EI}{l_b^2} + \frac{\mu L^2}{\pi^2} \quad (2)$$

where n is the coefficient corresponding to the end states of the needle (no units), E is the Young's Modulus of the needle material (N mm^{-2}), I is the moment of inertia of area of the needle (mm^4), l_b is the effective buckling length of the needle (mm), and μ is the spring stiffness of the tissue where the needle is pushed through (N m^{-1}). The needle will not buckle if the insertion force as described in

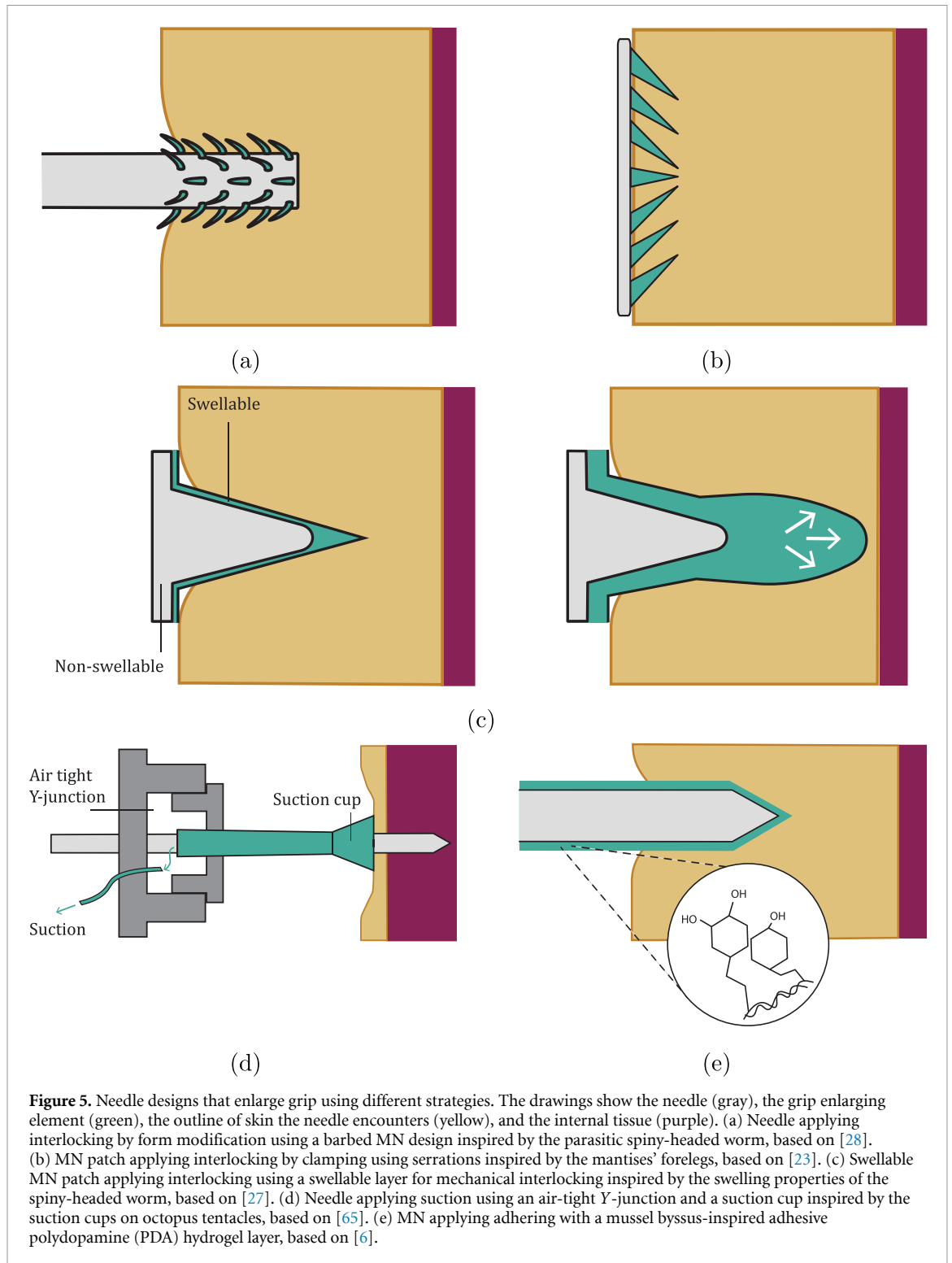
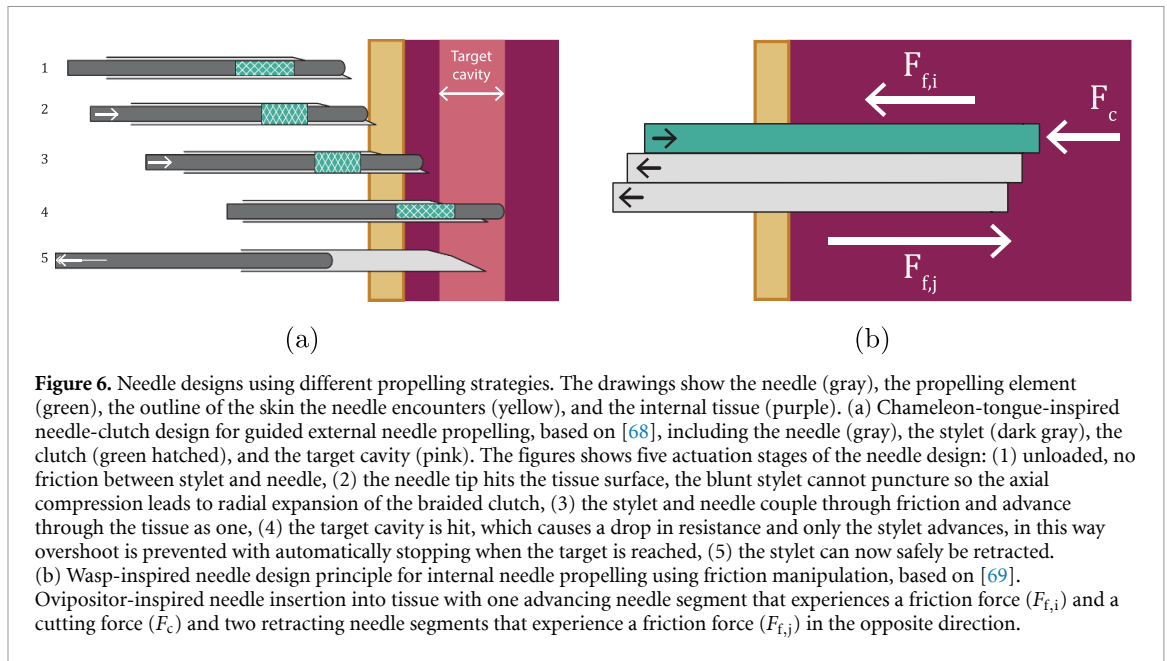


Figure 5. Needle designs that enlarge grip using different strategies. The drawings show the needle (gray), the grip enlarging element (green), the outline of skin the needle encounters (yellow), and the internal tissue (purple). (a) Needle applying interlocking by form modification using a barbed MN design inspired by the parasitic spiny-headed worm, based on [28]. (b) MN patch applying interlocking by clamping using serrations inspired by the mantises' forelegs, based on [23]. (c) Swellable MN patch applying interlocking using a swellable layer for mechanical interlocking inspired by the swelling properties of the spiny-headed worm, based on [27]. (d) Needle applying suction using an air-tight Y-junction and a suction cup inspired by the suction cups on octopus tentacles, based on [65]. (e) MN applying adhering with a mussel byssus-inspired adhesive polydopamine (PDA) hydrogel layer, based on [6].

equation (1) is lower than the buckling load ($P > F_i$). A smaller effective buckling length results in an increase in the buckling load, which means the needle can resist a higher insertion load. A smaller effective length was achieved by adding two support points to the guiding system, providing the needle two with fixed ends that double the buckling load. The needle is advanced cycle by cycle, similar to the lead-delivery system of a mechanical pencil. The authors proposed bellow tubes for a future needle

design that can extend and retract to allow drug delivery or blood extraction without hindering the needle motion [66]. A preliminary test without load was performed by ejecting the needle into air, which showed successful advancing of the needle with an extrusion length of 0.1 mm/cycle. A puncturing test in hydrogel agarose, as artificial skin, was performed successfully but showed an unintentional curvature in the needle path. The performed puncturing test in a PDMS elastomer sheet was unsuccessful, due to slipping at



the grasping component. A load-force test showed slipping at ± 0.011 N, while ± 0.078 N is needed for puncturing PDMS, which has characteristics resembling human skin.

Inspired by the chameleon's tongue, O'Cearbhaill *et al* [68] designed a needle with a radial mechanical clutch to prevent overshoot injuries in intravenous access, laparoscopic, and endo- and transluminal interventions. The radial clutch is formed by 16 biaxial stainless steel flat wires braided over a 1.1 mm diameter mandrel and crimped to a blunt rounded-tip stylet with 80 mm proximal and 50 mm distal length segments. This stylet-mounted clutch system is a universal design that is compatible with hypodermic or endoscopic needles. Here, it is assembled with a standard double-bevel, 100 mm length, 14- or 15-Gauge needle to compose the mechanical clutch needle. The chameleon's tongue has helical-wound collagen fibers in which the muscle extends axially to push the tongue forward. When compressed, the tongue is in tension and when triggered it extends to its relaxed conformation. The chameleon's tongue has a bony interior similar to the internal body of a needle and the helical wound fibers behave like biaxial braids that extend radially when compressed. Figure 6(a) shows the five actuation phases of the needle clutch. The design was tested in human cadavers and showed successful deployment through the peritoneum (i.e. the membrane that surrounds the abdominal organs) and successful needle disengagement from the stylet. In an *ex vivo* porcine test, the needle demonstrated successful emergency airway access when entering the trachea (i.e. the throat) and stopped before hitting the back wall, preventing tracheal or vocal chord damage. A test in porcine ear vein illustrated safe vascular access without the risk of damage due to puncturing through the target.

While the above examples use 'guidance' as the primary strategy for safe needle insertion, it is often combined with other strategies for grip reduction or enlargement. Liu *et al* [28] designed an insertion system added to the needle discussed in section 3.2.1 to have both stable needle insertion and tissue adherence.

4.2. Internal

4.2.1. Friction manipulation

Twenty-nine articles were collected presenting needles that use friction manipulation. Almost two-thirds of the needles were inspired by the parasitoid wasp, while the remainder were inspired by the mosquito. The parasitoid wasp has an ovipositor (i.e. an egg-laying organ) that consists of two or more valves connected with a dovetail interlocking mechanism that allows them to slide with respect to each other. The wasp advances one valve while retracting the other to move through wood to reach a host to inject eggs while reducing the risk of buckling. The mosquito uses a similar mechanism as the wasp in combination with vibration, which served as a source of inspiration for Izumi *et al* [48] and Suzuki *et al* [66] as described in section 3.1.2. The internal friction-manipulation strategy was mainly used for hypodermic needles, with medical applications such as blood extraction, biopsy, and focal therapy. However, most prototypes do not have a specific application yet and are designed for general percutaneous procedures.

One of the articles that describes a needle inspired by the ovipositor of the parasitoid wasp was written by Bloemberg *et al* [69] who developed a self-propelling needle for biopsy and focal laser ablation to treat prostate cancer (figure 6(b)). The needle system consists of a needle and a manual actuation unit that

drives the needle. The needle consists of six parallel 0.25 mm nitinol rods with a length of 200 mm and a total diameter of 0.8 mm connected at the tip by a heat shrink tube glued to one of the rods. The self-propelling motion is achieved by using the friction forces acting on the needle as described in section 1.1. By advancing one rod a certain distance while retracting the others a fifth of that distance, the friction force on the retracting rods overcomes the sum of the friction and cutting forces on the advancing rod. As a result, the needle moves forward step by step. *Ex vivo* tests in human prostate tissue inside a magnetic resonance imaging (MRI) system showed that the needle tip position was visible in the MR image and demonstrated successful propelling with zero external push of the needle, preventing large tissue motion and deformation. However, the measured slip ratio of 0.78–0.95 mm implies a large difference between the expected and true traveled distances of the needle.

Another needle that uses the principle of friction manipulation and used the parasitoid wasp as source of inspiration was developed by Frasson *et al* [70], they designed a steerable, multi-part, flexible needle for soft tissue interventions such as brain surgery. The needle consist of two interlocking segments that can move independently from each other, enabling the needle to be steered in a planar trajectory. Four prototypes were developed each with a length of 200 mm, a diameter of 12 mm or 9 mm, and a bevel-tip angle of 45° or 20°. Each needle segment contains two holes for securing the needle to mechanical transmission cables and two functional channels. One channel is for delivery or draining and the other contains an electro-magnetic tracking sensor that tracks the needle's position and orientation. To prevent buckling outside the tissue, the part of the needle that is not entering the tissue is supported by a trocar. The needle segments were 3D printed using the flexible rubber Digital Material™ DM 70shoreA, the tips were 3D printed using a more rigid material DM 95shoreA, to ensure a fixed bevel-tip without tip buckling. VeroWhite rigid plastic was added to the distal end of the needle to improve material toughness at the stress points where the mechanical transmission cables are connected. The interlocking segments of the needle allow it to be steered in a plane. The advanced segment becomes the leading segment and the offset between the segments creates an unsupported length that determines the deflection magnitude. Modifying this offset reorients the approach angle of the tip and thus controls the needle trajectory. The prototypes were evaluated in a gelatin phantom that replicates the canine brain, and different steering offsets were actuated via software. The evaluation showed an approximately linear relation between the curvature and steering offset. Furthermore, a smaller needle diameter resulted in a larger curvature but with greater planar

motion uncertainty. Lastly, a larger tip angle resulted in a larger curvature but also led to greater instability due to the forces acting on a smaller bevel-tip area.

The friction manipulation strategy is well-suited for steering due to the independent movement of the parallel needle segments. This is the only strategy that explores steering of the needle and the corresponding challenges due to the high compliancy and deformability of soft tissue. The needle designs are still prototypes with diameters varying between 12 mm [70, 71] and 0.03 mm [30] and number of needle segments varying between two [70, 72], three [30, 44, 48, 49], four [1, 71, 73–84], and six [3, 12, 67, 69].

5. Discussion

5.1. Comparative analysis

This review provides an overview of the working principles of bioinspired medical needles. The bioinspired needle designs can be classified based on how they modify the needle-tissue interaction and the propelling of the needle through the tissue. The needle design can modify the interaction with the tissue to serve two goals: (1) reducing the grip for smooth needle insertion and (2) enlarging the grip to resist needle retraction.

Figure 7(a) shows that the majority of the collected articles present bioinspired medical needles that use either translation as an active strategy or form modification as a passive strategy to reduce grip. Translation as one of the most frequently described strategies might be related to it not only being used as main strategy in the form of vibration, but also for friction manipulation. Form modification as one of the most frequently described strategies may be correlated to the upward trend of additive manufacturing in medical devices [85], since the needle form is often modified using 3D printing. Only a few articles (i.e. two articles) were found describing needles that use rotation as a strategy. This may be because rotating the needle focuses more on the actuation instead of the design of the needle itself. There may be opportunities in exploring the use of rotation techniques in needle design, by taking inspiration from the boring techniques of shipworms or the ovipositors of locusts.

The enlarging grip strategy was mainly used in MN patches that need to attach to the skin for a longer period of time. Figure 7(a) shows that the majority of collected articles use interlocking as a strategy to enlarge grip. This result may be explained by the abundance of interlocking features in nature. In addition, since interlocking is mainly realized through form modification, the same explanation of the upward trend in additive manufacturing as for passive form modification applies. An interesting finding is that the most common method of form modification is adding barbs, which is both used to reduce grip in a passive way and enlarge grip through

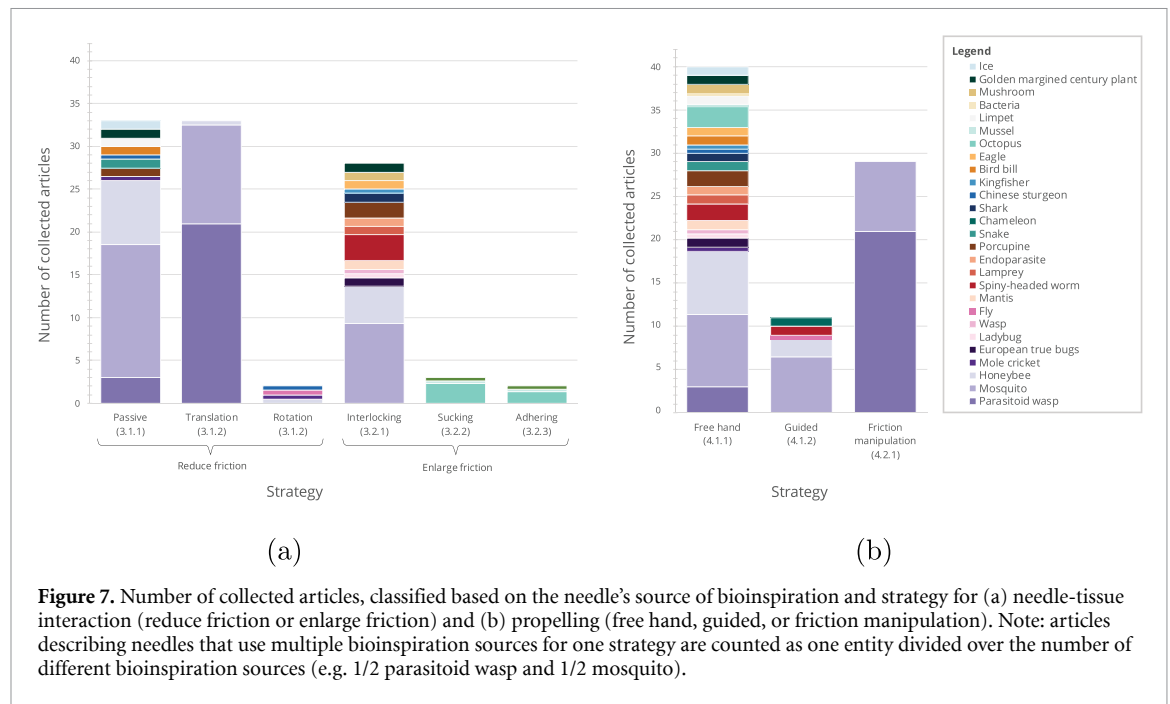


Figure 7. Number of collected articles, classified based on the needle's source of bioinspiration and strategy for (a) needle-tissue interaction (reduce friction or enlarge friction) and (b) propelling (free hand, guided, or friction manipulation). Note: articles describing needles that use multiple bioinspiration sources for one strategy are counted as one entity divided over the number of different bioinspiration sources (e.g. 1/2 parasitoid wasp and 1/2 mosquito).

interlocking. In nature, this method is seen in animals and plants. The smallest number of collected articles (i.e. three articles) describe needles using sucking and adhering as a strategy to enlarge grip. One could speculate that this is due to the fact that only the octopus was used as a source of inspiration and the complexity of its suction cup. Other organisms could be explored, such as the mouth of tadpoles or the water management system of tree roots. The lamprey's mouth, for instance, is used for interlocking and also has sucking capabilities.

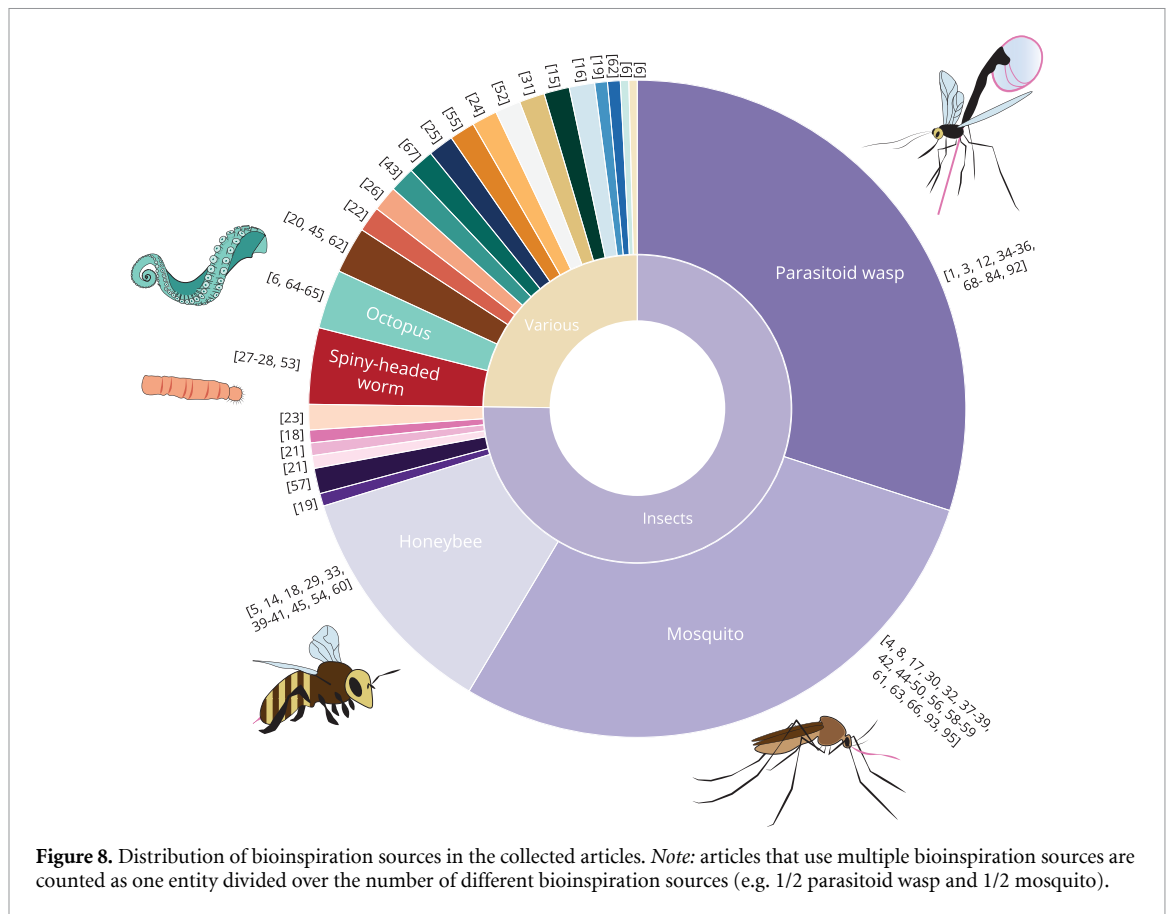
The results of the classification based on propelling show that the majority of collected articles describe needles that implement free-hand insertion (figure 7(b)). This may be explained by the fact that most needles have not (yet) implemented a needle propelling strategy. Friction manipulation is the second largest propelling group which correlates with translation being the largest interacting group, since friction-manipulation and translation strategies are often applied together. It is possible that there are alternative ways to manipulate friction without using translation. As for now, only friction manipulation is used as a strategy to implement steering, but it may be possible that alternative bioinspired strategies for steering exist. Surprisingly, guided needles are the smallest group, this could have the same explanation as above that most articles did not consider the needle propelling design yet. Another possible explanation could be that a guidance system is designed separately (i.e. excluding the needle).

In almost all collected articles, a combination of strategies was used to improve the needle design. In nature, multiple strategies are often combined as well, for example the mosquito that first anchors into the skin and then advances by using friction

manipulation and vibration. In general, further research is needed to determine the optimal combination(s) of needle-tissue interaction and propelling strategies for different medical applications.

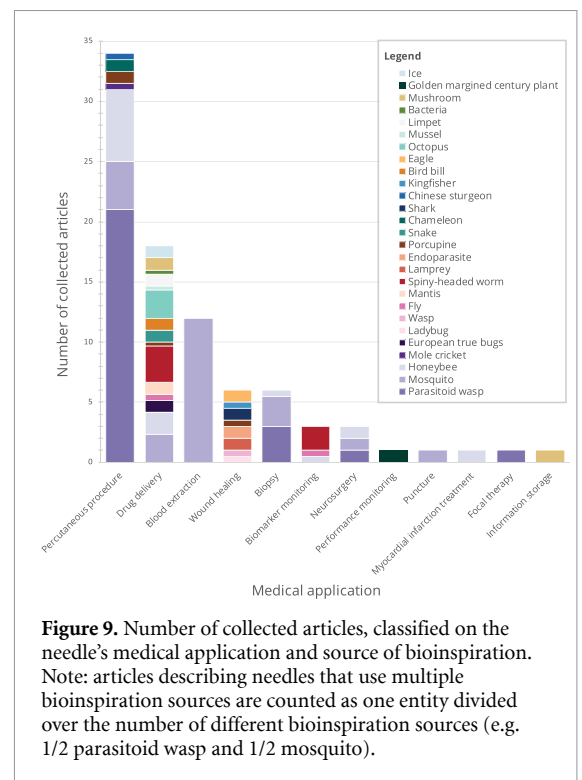
Figure 8 shows that the main sources of bioinspiration are insects (indicated by the purple-tinted colors), which may be due to the presence of needle-like stingers in many insects. Another common source of inspiration is parasites, which may be related to their infiltrating characteristics. An interesting finding is that for the translation strategy, only insects were used as source of inspiration, while for interlocking a wider variety of bioinspiration sources was used. These result may partially be explained by the many varieties in nature that can be found using interlocking strategies. Overall, animals were more commonly used as a source of inspiration than other organisms such as plants or fungi. However, these other organisms also offer a variety of interesting strategies and shapes worth exploring.

Among the collected articles, additive manufacturing is the most commonly used manufacturing method, with 33 out of 80 articles utilizing some form of 3D printing. Within the 3D printing techniques used, UV lithography with photoresin is particularly prevalent due to its high precision. Other 3D printing techniques include material extrusion and magneto-rheological drawing lithography, with material choices depending on the specific 3D printing method, this results in plastics being the most commonly used material. Moulding is the second most common manufacturing method and is used in 15 out of 80 articles. The moulds were commonly made out of PDMS, although metal moulds made from aluminum were also used. Silk fibroin, silicon or hydrogel were used to fill the mould and were

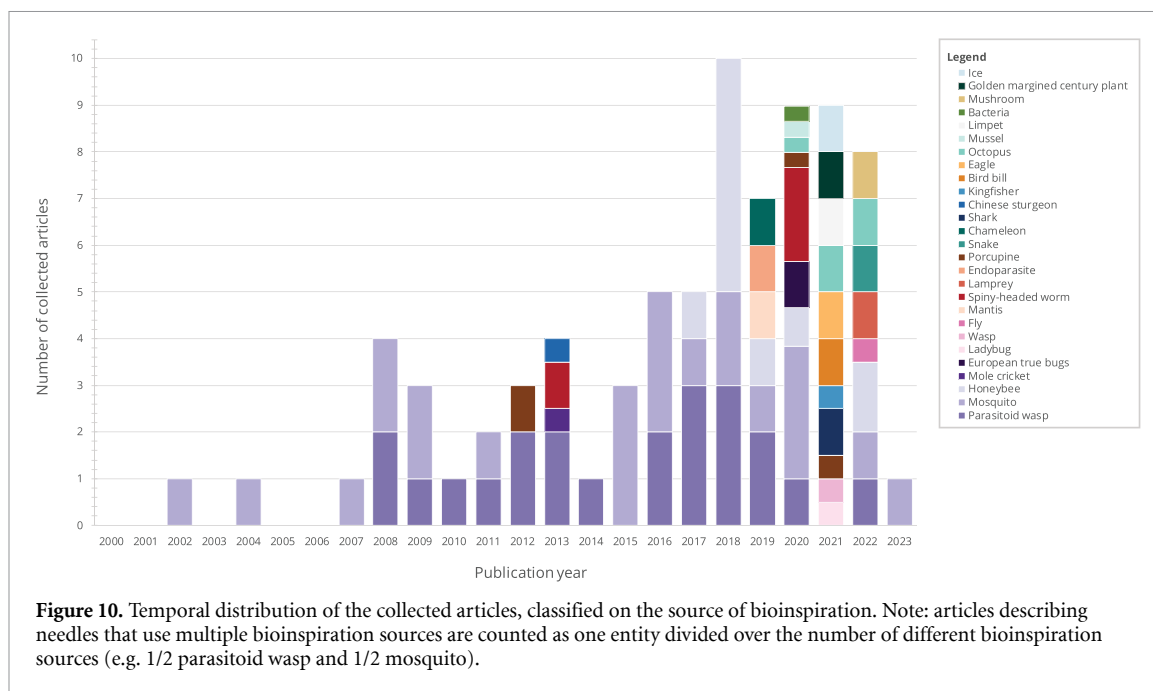


cured with an UV light. Another technique that is utilized in 12 out of 80 articles is removing material via laser cutting or etching. Lastly, 12 out of 80 articles used off-the-shelf parts assembled into the final prototype, with some parts modified by laser cutting. The material choices depended on the desired properties of the needle design and the employed manufacturing method. For flexible designs, rubber was often chosen while for designs that needed more strength, ceramics and metals were used. Some articles specifically focused on material and manufacturing method selection, such as Schneider *et al* [36], who explored different manufacturing methods and corresponding materials. A few articles only included a computer-simulated model of the needle, rather than a manufactured design.

Most of the collected articles did not define a specific medical application and were designed for general percutaneous procedures (figure 9). This is likely because most of the designs are still in the prototype phase and are not yet commercially available. While designing for a general purpose may be beneficial to create widely applicable needles, designing for a specific medical application can be beneficial when optimizing for a task. Drug delivery is the largest specific medical application of MN patches, as they are primarily designed for this purpose. Since it is important to stay attached to the skin during drug delivery, the main strategy is grip enlargement



for which a variety of bioinspiration sources was used. Interesting to note is that mosquitoes are the only organisms used as inspiration for blood extraction applications, likely due to their blood-sucking



abilities. Further research should be undertaken to investigate the potential of other bloodsucking organisms and their usability for this medical application.

5.2. Limitations and recommendations

A systematic approach was employed to increase the likelihood of identifying relevant bioinspired needle designs. Nevertheless, it is possible that relevant articles on bioinspired medical needles were missed due to, for instance, missing relevant keywords. The literature search was conducted using general terms such as bioinspiration rather than specific organisms. Snowballing resulted in additional articles with titles including ‘mosquito-inspired needle’. Therefore, it is likely that there are other insect-inspired terms used in article titles that were not found when using the more general keyword ‘bioinspiration.’

As already stated by Rahamim and Azagury [86] there should be a general use of bioinspiration terms to prevent misuse or disuse of the term, moreover it can increase the audience and progress of the field. It is possible that the collected articles are not representing the entire field, as a large number of the articles were published by the same research groups and contain developments on previous publications of the same prototype. Additionally, only a limited number of databases (i.e. Scopus, WoS, and PubMed) was used for the reproducibility of this study. Furthermore, the articles were manually selected following the eligibility criteria, however, manual selection is always biased due to the interpretation of the criteria.

It might be difficult to draw conclusions about which strategy is most effective based on the results published in different articles. The test set-ups varied among articles, for instance, in some articles needles

were tested *ex vivo* on porcine skin or organ tissue, while others were tested *in vivo* on mice or *in vitro* on tissue phantoms made of PVC or silicon. The measured variables of the tests varied as well; some articles reported the reduced insertion forces, while others reported the durability or drug distribution.

An interesting direction for future research is the use of biomaterials for the needle design, such as Yoshida and Takei [87], who designed a needle from a human hair or Olatunji *et al* [88], who created a needle from fish scales. A second interesting direction is the use of biological processes, such as Gao *et al* [89], who used bioinspired crystallization for the needle design. In addition to investigating needles themselves, it may be useful to consider robotic needle systems. Zhang *et al* [90] showed a robotic needle system design based on a leech, this system, rather than steering the needle to the target, moves the tissue, and thus the target, to the sucking arm. For grip-enlarging strategies, it may be useful to examine gripper designs instead of needle designs. There were only three articles collected describing needle designs using suction and adhesion strategies. These needle designs have significant overlap with medical gripper designs. Therefore, medical gripper designs could potentially be integrated with needles as demonstrated by Joymungul *et al* [65].

5.3. Temporal distribution and future perspective

The design of medical needles using bioinspiration is a relatively new field, with the first article on the topic being published in 2002. Figure 10 shows an increasing number of publications concerning bioinspired needles over the last 20 years. Not only the quantity has increased, also the variety of the used bioinspiration sources has increased. During the first 15 years,

bioinspiration for needle design was largely limited to the parasitoid wasp and mosquito. However, in the past 4 years, a variety of over 25 species has been investigated, and this trend is likely to continue in the future. The adhering and sucking strategies appeared in 2020 and 2021, thus we can expect that especially those strategies will develop in the future. However, it is important to note that the included articles consider prototypes that are not yet suitable for clinical practice. This is particularly evident in the fabrication methods, where as stated before 3D printing is most commonly used. While 3D printing is useful for prototyping, it is not suitable for high-volume production due to its high costs. More suitable production methods include the use of moulds such as ferrofluid moulding as used by Zhang *et al* [23]. The development of production techniques will enable the development of bioinspired needles and fabrication of needles in their required shape.

The implementation of bioinspired needles in clinical practice is expected to take time due to the need of thorough testing and compliance with healthcare regulations. However, it is likely that bioinspired needles will become a less painful and more accurate alternative to current hypodermic needles and MN patches. Additionally, MN patches might be used as wearable drug delivery systems for conditions such as diabetes.

6. Conclusion

This review provides a comprehensive overview of the current developments in bioinspired needles for medical applications. A scientific literature search of bioinspired needles was conducted using Scopus, WoS, and PubMed. In total, 80 articles were included and classified according to their needle-tissue interaction and needle propulsion. The needle-tissue interaction can be modified to reduce or enlarge grip. Passive and active strategies were identified to reduce grip, including form modification, translation, and rotation. Among them, form modification was the most commonly used. To increase grip, interlocking,

sucking, and adhering strategies were identified, with interlocking being the most common. External needle propulsion strategies include free hand and guided, with free hand being the most common, but lacking a bioinspired aspect. Internal propelling could be achieved through friction manipulation of the tissue. Multiple strategies can be combined to design an optimal needle for accurate targeting, minimal tissue damage, and pain reduction, surpassing conventional hypodermic needles and MN patches. While these designs are still in developmental stages, they provide ample opportunity for designers to improve existing prototypes or draw inspiration from these strategies to create a new generation of bioinspired needles that could have a significant impact on the medical world.

Data availability statement

All data that support the findings of this study are included within the article (and any supplementary files).

Acknowledgments

This work was supported by the Netherlands Organisation for Scientific Research (Nederlandse Organisatie voor Wetenschappelijk Onderzoek, NWO), domain Applied and Engineering Sciences (TTW), and which is partly funded by the Ministry of Economic Affairs. Grant number 80450, Perspectief programme, Photonics Translational Research—Medical Photonics (MEDPHOT), awarded to PB. URL: www.nwo.nl/. The funders had no role in study design, data collection and analysis, decision to publish, or preparation of the manuscript.

Appendix A. Search queries

In this appendix, the search queries used for the Scopus, WoS, and PubMed databases are displayed in table A1.

Table A1. Search queries for Scopus, WoS, and PubMed databases.

| Database | Query |
|----------|--|
| Scopus | TITLE-ABS-KEY ((bio-inspir* OR bioinspir* OR “Biolog* inspire*” OR biomim* OR “Nature inspir*” OR Nature-inspir* OR bionic*) AND (*needle*)) AND (LIMIT-TO (LANGUAGE , “English”)) AND (EXCLUDE (DOCTYPE, “cr”)) |
| WoS | TS = ((bio-inspir* OR bioinspir* OR “Biolog* inspire*” OR biomim* OR “Nature inspir*” OR Nature-inspir* OR bionic*) AND (*needle*)) Refined By: Languages: English |
| PubMed | (bioinspir* [Title/Abstract] OR “Biolog* inspire*” [Title/Abstract] OR biomim* [Title/Abstract] OR “Nature inspir*” [Title/Abstract] OR bionic* [Title/Abstract]) AND (*needle* [Title/Abstract]) |

Appendix B. Tables of the classifications based on needle-tissue interaction and propelling

In this appendix, the collected articles are displayed, where table B1 shows the articles presenting needle designs that aim to reduce

or enlarge grip and table B2 shows the articles presenting needle designs that alter the needle propulsion.

Table B1. Classification of grip enlarging and reduction strategies for bioinspired needles. Author(s), year of publication, key application(s), source(s) of bioinspiration, corresponding category in the classification of the collected articles, needle outer diameter, needle length, and evaluation stage, where 0 indicates a mechanical strength test, 1 indicates tested by computer simulation, 2 indicates tested in tissue phantom, 3 indicates tested *ex vivo* on animal tissue and 4 indicates tested *in vivo* on animal tissue. n/a = not available. *estimated value.

| Author | Pub. Year | Medical application | Bioinspiration | Classification | Needle diameter [mm] | Needle length [mm] | Eval. stage |
|-----------------------|-----------|-------------------------------------|-------------------------------|---------------------------|----------------------|--------------------|-------------|
| Aoyagi et al [32] | 2008 | Percutaneous procedure | Mosquito | Form; Translation | 0.09 – 0.23 | 1* | 1, 2 |
| Bloemberg et al [69] | 2022 | Biopsy, Focal therapy | Parasitoid wasp | Translation | 0.84 | 200 | 3 |
| Burrows et al [91] | 2017 | Percutaneous procedure | Parasitoid wasp | Translation | 4 | 300 | 2 |
| Burrows et al [74] | 2013 | Percutaneous procedure | Parasitoid wasp | Translation | 8 | 200 | 1 |
| Cai et al [18] | 2022 | Drug delivery, Biomarker monitoring | Honeybee | Rotation | 0.21 | 1.2 | 1, 3 |
| Chen et al [29] | 2018 | Percutaneous procedure | Honeybee | Form, Interlocking | 0.2 | 2 | 1, 3 |
| Chen et al [33] | 2018 | Drug delivery | Honeybee | Form, Interlocking | 0.3* | 1.4* | 3 |
| Cho et al [20] | 2012 | Percutaneous procedure | Porcupine | Form, Interlocking | 0.6* | 2.5* | 2, 3 |
| Deng et al [22] | 2022 | Wound healing | Lamprey | Interlocking | 1.5* | 1.5, 2.5 | 3, 4 |
| Frasson et al [34] | 2008 | Percutaneous procedure | Parasitoid wasp | Form | 4.4 | 80 | 3 |
| Frasson et al [35] | 2008 | Percutaneous procedure | Parasitoid wasp | Form | 4.4* | 80* | 3 |
| Frasson et al [92] | 2010 | Percutaneous procedure | Parasitoid wasp | Translation | 4.4 | 120* | 3 |
| Frasson et al [70] | 2012 | Percutaneous procedure | Parasitoid wasp | Translation | 9, 12 | 200 | 2 |
| Fu et al [64] | 2022 | Drug delivery | Octopus | Sucking | 0.45* | 0.6* | 3, 4 |
| Gidde et al [39] | 2020 | Biopsy | Honeybee, Mosquito | Form, Translation | 4 | 180 | 2, 3 |
| Gidde et al [37] | 2022 | Percutaneous procedure | Mosquito | Form, Translation | 3 | 180 | 3 |
| Gidde et al [38] | 2023 | Percutaneous procedure | Mosquito | Form, Translation | 3 | 180 | 2 |
| Giovannini et al [42] | 2017 | Biopsy | Mosquito | Form | 2.4 | 3.84* | 2 |
| Sravani et al [43] | 2022 | Drug delivery | Snake | Form | 0.08 | 0.75 | 1 |
| Gittard et al [44] | 2009 | Drug delivery | Mosquito | Form, Interlocking | 0.032 | 0.5 | n/a |
| Guo et al [25] | 2021 | Wound healing | Shark | Interlocking | 0.6 | 1 | 4 |
| Han et al [45] | 2020 | Drug delivery | Mosquito, Honeybee, Porcupine | Interlocking | 0.4 | 4 | 2, 3 |
| Hara et al [47] | 2016 | Blood extraction | Mosquito | Form | 0.07 | 2.2 | n/a |
| Hara et al [46] | 2016 | Blood extraction | Mosquito | Form | 0.05 | 5 | 2 |
| Izumi et al [48] | 2008 | Blood extraction | Mosquito | Translation, Interlocking | 0.06 | 1 | 2 |
| Izumi et al [30] | 2009 | Percutaneous procedure | Mosquito | Interlocking | 0.03 | 1* | 2 |
| Izumi et al [49] | 2011 | Blood extraction | Mosquito | Translation, Interlocking | 0.03 | 1 | 2 |

(Continued.)

Table B1. (Continued.)

| Author | Pub. Year | Medical application | Bioinspiration | Classification | Needle diameter [mm] | Needle length [mm] | Eval. stage |
|-------------------------------------|-----------|--------------------------------------|-------------------------------|--------------------|----------------------|--------------------|-------------|
| Jeon <i>et al</i> [26] | 2019 | Wound healing | Endoparasite | Interlocking | 0.25 | 0.75 | 3, 4 |
| Joymungul <i>et al</i> [65] | 2021 | Drug delivery | Octopus | Sucking, Adhering | 1.08 | 260* | 3 |
| Kim <i>et al</i> [8] | 2018 | Drug delivery | Mosquito | Translation | 0.06-0.14 | 5 | 3 |
| Ko and Rodriguez y Baena [76] | 2012 | Percutaneous procedure | Parasitoid wasp | Translation | 12 | 200 | 2 |
| Ko <i>et al</i> [71] | 2011 | Percutaneous procedure | Parasitoid wasp | Translation | 12 | 200 | 2 |
| Ko <i>et al</i> [72] | 2013 | Percutaneous procedure | Parasitoid wasp | Translation | 4 | 180 | 1 |
| Leibinger <i>et al</i> [77] | 2016 | Percutaneous procedure | Parasitoid wasp | Translation | 4 | 200 | 2 |
| Li <i>et al</i> [93] | 2019 | Neurosurgery | Mosquito | Form, Interlocking | 0.5 | 18 | 1 |
| Li <i>et al</i> [50] | 2020 | Biopsy | Mosquito | Interlocking | 1 | 20* | 2 |
| Li <i>et al</i> [52] | 2021 | Drug delivery | Limpet | Form | 0.05-0.2 | 0.5 | 2, 4 |
| Li <i>et al</i> [15] | 2021 | Performance monitoring | Golden margined century plant | Form, Interlocking | 0.35* | 2 | 2, 4 |
| Li <i>et al</i> [31] | 2022 | Drug delivery, Information storage | Mushroom | Interlocking | 0.2-0.6 | 0.6-1 | 3, 4 |
| Liu <i>et al</i> [28] | 2020 | Drug delivery, Biomarker monitoring | Spiny-headed worm | Interlocking | 0.108 | 1 | 3 |
| Liu <i>et al</i> [53] | 2020 | Drug delivery, Biomarker monitoring | Spiny-headed worm | Interlocking | 0.09* | 0.26 | 0 |
| Lu <i>et al</i> [54] | 2022 | Myocardial infarction treatment | Honeybee | Interlocking | 0.25 | 3 | 2, 3, 4 |
| Matheson and Rodriguez y Baena [78] | 2020 | Percutaneous procedure | Parasitoid wasp | Translation | 2.5 | n/a | 2 |
| Matheson <i>et al</i> [1] | 2018 | Percutaneous procedure | Parasitoid wasp | Translation | 2.5 | 100* | 1 |
| Matheson <i>et al</i> [79] | 2019 | Percutaneous procedure | Parasitoid wasp | Translation | 2.5 | 120* | 1 |
| Mizuno <i>et al</i> [55] | 2021 | Drug delivery | Bird bill | Form | 0.5 | 0.9 | 3, 4 |
| Oka <i>et al</i> [56] | 2002 | Blood extraction | Mosquito | Form | 0.085 | 1 | 2 |
| Oldfield <i>et al</i> [80] | 2014 | Percutaneous procedure | Parasitoid wasp | Translation | 6 | 100 | 2 |
| Oldfield <i>et al</i> [81] | 2015 | Biopsy | Parasitoid wasp | Translation | 4.00 | n/a | 1 |
| Plamadeala <i>et al</i> [57] | 2020 | Drug delivery | European true bugs | Interlocking | 0.0097 | 0.0397 | 3 |
| Sahlabadi and Hutapea [14] | 2018 | Percutaneous procedure | Honeybee | Form | 1-3 | 180 | 2, 3 |
| Sahlabadi and Hutapea [40] | 2018 | Percutaneous procedure | Honeybee | Form | 3 | 180 | 2 |
| Sahlabadi <i>et al</i> [5] | 2017 | Percutaneous procedure, Neurosurgery | Honeybee | Form | 3 | 180* | 2, 3 |

(Continued.)

Table B1. (Continued.)

| Author | Pub. Year | Medical application | Bioinspiration | Classification | Needle diameter [mm] | Needle length [mm] | Eval. stage |
|------------------------------|-----------|------------------------|--------------------------------|---------------------------------|----------------------|--------------------|-------------|
| Sahlabadi <i>et al</i> [41] | 2018 | Percutaneous procedure | Honeybee | Form | 3 | 180 | 3 |
| Scali <i>et al</i> [12] | 2017 | Percutaneous procedure | Parasitoid wasp | Translation | 1.55 | 250 | 2 |
| Scali <i>et al</i> [3] | 2017 | Percutaneous procedure | Parasitoid wasp | Translation | 1.2 | 160 | 2 |
| Scali <i>et al</i> [67] | 2019 | Percutaneous procedure | Parasitoid wasp | Translation | 0.8, 0.6, 0.4 | 390 | 2 |
| Schneider <i>et al</i> [36] | 2009 | Neurosurgery, Biopsy | Parasitoid wasp | Form | 4* | 90* | 3 |
| Secoli <i>et al</i> [82] | 2018 | Percutaneous procedure | Parasitoid wasp | Translation | 8 | 200 | 2 |
| Sprang <i>et al</i> [73] | 2016 | Percutaneous procedure | Parasitoid wasp | Translation | 2 | 200 | 2 |
| Suzuki <i>et al</i> [17] | 2015 | Blood extraction | Mosquito | Form, Translation, Interlocking | 0.1 | 1 | 2 |
| Suzuki <i>et al</i> [4] | 2015 | Blood extraction | Mosquito | Form, Translation, Interlocking | 0.1 | 1 | 2 |
| Suzuki <i>et al</i> [59] | 2015 | Blood extraction | Mosquito | Form, Translation, Interlocking | 0.06 | 2 | 2 |
| Suzuki <i>et al</i> [58] | 2018 | Blood extraction | Mosquito | Form, Translation, Interlocking | 0.05 | 1 | 2 |
| Suzuki <i>et al</i> [66] | 2020 | Puncture | Mosquito | Translation | 0.1 | 4 | 2 |
| Tran <i>et al</i> [60] | 2019 | Percutaneous procedure | Honeybee | Form, Interlocking | 0.38 | 1.3 | 2 |
| Tsuchiya <i>et al</i> [61] | 2007 | Blood extraction | Mosquito | Form | 0.05 | n/a | 1 |
| Velivela <i>et al</i> [62] | 2021 | Wound healing | Kingfisher, Porcupine | Interlocking | 0.58 | 3.9 | 1 |
| Viridyawan and Y Baena [84] | 2018 | Percutaneous procedure | Parasitoid wasp | Translation | 2.5 | n/a | 2 |
| Viridyawan <i>et al</i> [83] | 2018 | Percutaneous procedure | Parasitoid wasp | Translation | 4 | n/a | 2 |
| Wang <i>et al</i> [63] | 2016 | Percutaneous procedure | Mosquito | Form | n/a | n/a | 1 |
| Wang and Cong [19] | 2013 | Percutaneous procedure | Mole cricket, Chinese sturgeon | Form, Rotation | 1.6 | 30* | 2 |
| Yang <i>et al</i> [27] | 2013 | Drug delivery | Endoparasite | Interlocking | 0.28 | 0.7 | 3 |
| Zhang <i>et al</i> [23] | 2019 | Drug delivery | Mantis | Interlocking | 0.25 | 0.6 | 3, 4 |
| Zhang <i>et al</i> [6] | 2020 | Drug delivery | Bacteria, Mussel, Octopus | Sucking | 0.3 | 0.6 | 3, 4 |
| Zhang <i>et al</i> [21] | 2021 | Wound healing | Wasp, Ladybug | Interlocking | 0.6* | 1* | 3 |
| Zhang <i>et al</i> [24] | 2021 | Wound healing | Eagle | Interlocking | 0.41 | 0.75 | 3, 4 |
| Zhang <i>et al</i> [16] | 2021 | Drug delivery | Ice | Form | 0.5 | 0.88 | 2, 3, 4 |

Table B2. Classification of external and internal propelling strategies for bioinspired needles. Author(s), year of publication, key application(s), source(s) of bioinspiration, and corresponding category in the classification of the collected articles.

| Author | Publication Year | Medical application | Bioinspiration | Classification |
|-------------------------------------|------------------|--|----------------------------------|-----------------------|
| Aoyagi <i>et al</i> [32] | 2008 | Blood extraction | Mosquito | Free hand |
| Bloemberg <i>et al</i> [69] | 2022 | Biopsy, Focal therapy | Parasitoid wasp | Friction manipulation |
| Burrows <i>et al</i> [91] | 2017 | Percutaneous procedure | Parasitoid wasp | Friction manipulation |
| Burrows <i>et al</i> [74] | 2013 | Percutaneous procedure | Parasitoid wasp | Friction manipulation |
| Cai <i>et al</i> [18] | 2022 | Drug delivery, Biomarker monitoring | Honeybee, Fly | Guided |
| Chen <i>et al</i> [29] | 2018 | Percutaneous procedure | Honeybee | Free hand |
| Chen <i>et al</i> [94] | 2018 | Drug delivery | Honeybee | Free hand |
| Cho <i>et al</i> [20] | 2012 | Percutaneous procedure | Porcupine | Free hand |
| Deng <i>et al</i> [22] | 2022 | Wound healing | Lamprey | Free hand |
| Frasson <i>et al</i> [92] | 2010 | Percutaneous procedure | Parasitoid wasp | Friction manipulation |
| Frasson <i>et al</i> [35] | 2008 | Percutaneous procedure | Parasitoid wasp | Free hand |
| Frasson <i>et al</i> [34] | 2008 | Percutaneous procedure | Parasitoid wasp | Free hand |
| Frasson <i>et al</i> [70] | 2012 | Percutaneous procedure | Parasitoid wasp | Friction manipulation |
| Fu <i>et al</i> [64] | 2022 | Drug delivery | Octopus | Free hand |
| Gidde <i>et al</i> [39] | 2020 | Biopsy | Honeybee, Mosquito | Guided |
| Gidde <i>et al</i> [37] | 2022 | Percutaneous procedure | Mosquito | Guided |
| Gidde <i>et al</i> [38] | 2023 | Percutaneous procedure | Mosquito | Guided |
| Giovannini <i>et al</i> [42] | 2017 | Biopsy | Mosquito | Free hand |
| Sravani <i>et al</i> [43] | 2022 | Drug delivery | Snake | Free hand |
| Gittard <i>et al</i> [44] | 2009 | Drug delivery | Mosquito | Friction manipulation |
| Guo <i>et al</i> [25] | 2021 | Wound healing | Shark | Free hand |
| Han <i>et al</i> [45] | 2020 | Drug delivery | Mosquito, Honeybee, Porcupine | Free hand |
| Hara <i>et al</i> [46] | 2016 | Blood extraction | Mosquito | Free hand |
| Hara <i>et al</i> [47] | 2016 | Blood extraction | Mosquito | Free hand |
| Izumi <i>et al</i> [49] | 2011 | Blood extraction | Mosquito | Friction manipulation |
| Izumi <i>et al</i> [30] | 2009 | Percutaneous procedure | Mosquito | Friction manipulation |
| Izumi <i>et al</i> [48] | 2008 | Blood extraction | Mosquito | Friction manipulation |
| Jeon <i>et al</i> [26] | 2019 | Wound healing | Endoparasite | Free hand |
| Joymungul <i>et al</i> [65] | 2021 | Drug delivery | Octopus | Free hand |
| Kim <i>et al</i> [8] | 2018 | Drug delivery | Mosquito | Free hand |
| Ko <i>et al</i> [71] | 2011 | Percutaneous procedure | Parasitoid wasp | Friction manipulation |
| Ko and Rodriguez y Baena [76] | 2012 | Percutaneous procedure | Parasitoid wasp | Friction manipulation |
| Ko <i>et al</i> [72] | 2013 | Percutaneous procedure | Parasitoid wasp | Friction manipulation |
| Leibinger <i>et al</i> [77] | 2016 | Percutaneous procedure | Parasitoid wasp | Friction manipulation |
| Li <i>et al</i> [50] | 2020 | Biopsy | Mosquito | Guided |
| Li <i>et al</i> [93] | 2019 | Neurosurgery | Mosquito | Free hand |
| Li <i>et al</i> [31] | 2022 | Drug delivery, Information storage | Mushroom | Free hand |
| Li <i>et al</i> [52] | 2021 | Drug delivery | Limpet | Free hand |
| Li <i>et al</i> [15] | 2021 | Performance monitoring | Golden margined century plant | Free hand |
| Liu <i>et al</i> [28] | 2020 | Drug delivery, Biomarker monitoring | Spiny-headed worm | Free hand |
| Liu <i>et al</i> [53] | 2020 | Drug delivery, Biomarker monitoring | Spiny-headed worm | Guided |
| Lu <i>et al</i> [54] | 2022 | Myocardial infarction treatment | Honeybee | Free hand |
| Matheson and Rodriguez y Baena [78] | 2020 | Percutaneous procedure | Parasitoid wasp | Friction manipulation |
| Matheson <i>et al</i> [79] | 2019 | Percutaneous procedure | Parasitoid wasp | Friction manipulation |
| Matheson <i>et al</i> [1] | 2018 | Percutaneous procedure | Parasitoid wasp | Friction manipulation |
| Mizuno <i>et al</i> [55] | 2021 | Drug delivery | Bird bill | Free hand |
| O'Ceirbhail <i>et al</i> [68] | 2019 | Percutaneous procedure | Chameleon | Guided |
| Oka <i>et al</i> [56] | 2002 | Blood extraction | Mosquito | Free hand |
| Oldfield <i>et al</i> [80] | 2014 | Percutaneous procedure | Parasitoid wasp | Friction manipulation |

(Continued.)

Table B2. (Continued.)

| Author | Publication Year | Medical application | Bioinspiration | Classification |
|----------------------------|------------------|--------------------------------------|--------------------------------|-----------------------|
| Oldfield et al [81] | 2015 | Biopsy | Parasitoid wasp | Friction manipulation |
| Plamadeala et al [57] | 2020 | Drug delivery | European true bugs | Free hand |
| Sahlabadi and Hutapea [40] | 2018 | Percutaneous procedure | Honeybee | Free hand |
| Sahlabadi et al [41] | 2018 | Percutaneous procedure | Honeybee | Guided |
| Sahlabadi et al [5] | 2017 | Percutaneous procedure, Neurosurgery | Honeybee | Free hand |
| Sahlabadi and Hutapea [14] | 2018 | Percutaneous procedure | Honeybee | Free hand |
| Scali et al [3] | 2017 | Percutaneous procedure | Parasitoid wasp | Friction manipulation |
| Scali et al [67] | 2019 | Percutaneous procedure | Parasitoid wasp | Friction manipulation |
| Scali et al [12] | 2017 | Percutaneous procedure | Parasitoid wasp | Friction manipulation |
| Schneider et al [36] | 2009 | Neurosurgery, Biopsy | Parasitoid wasp | Free hand |
| Secoli et al [82] | 2018 | Percutaneous procedure | Parasitoid wasp | Friction manipulation |
| Sprang et al [73] | 2016 | Percutaneous procedure | Parasitoid wasp | Friction manipulation |
| Suzuki et al [59] | 2015 | Blood extraction | Mosquito | Friction manipulation |
| Suzuki et al [17] | 2015 | Blood extraction | Mosquito | Friction manipulation |
| Suzuki et al [58] | 2018 | Blood extraction | Mosquito | Friction manipulation |
| Suzuki et al [4] | 2015 | Blood extraction | Mosquito | Friction manipulation |
| Suzuki et al [66] | 2020 | Puncture | Mosquito | Guided |
| Tran et al [60] | 2019 | Percutaneous procedure | Honeybee | Free hand |
| Tsuchiya et al [95] | 2004 | Blood extraction | Mosquito | Guided |
| Tsuchiya et al [61] | 2007 | Blood extraction | Mosquito | Guided |
| Velivela et al [62] | 2021 | Wound healing | Kingfisher, Porcupine | Free hand |
| Virdyawan et al [83] | 2018 | Percutaneous procedure | Parasitoid wasp | Friction manipulation |
| Virdyawan and Y Baena [84] | 2018 | Percutaneous procedure | Parasitoid wasp | Friction manipulation |
| Wang and Cong [19] | 2013 | Percutaneous procedure | Mole cricket, Chinese sturgeon | Free hand |
| Wang et al [63] | 2016 | Percutaneous procedure | Mosquito | Free hand |
| Yang et al [27] | 2013 | Drug delivery | Spiny-headed worm | Free hand |
| Zhang et al [21] | 2021 | Wound healing | Wasp, Ladybug | Free hand |
| Zhang et al [24] | 2021 | Wound healing | Eagle | Free hand |
| Zhang et al [23] | 2020 | Drug delivery | Bacteria, Mussel, Octopus | Free hand |
| Zhang et al [6] | 2019 | Drug delivery | Mantis | Free hand |
| Zhang et al [16] | 2021 | Drug delivery | Ice | Free hand |

ORCID iDs

Zola Fung-A-Jou  <https://orcid.org/0000-0002-7478-6785>

Jette Bloemberg  <https://orcid.org/0000-0002-6627-4165>

References

- Matheson E, Watts T, Secoli R and Rodriguez y Baena F 2018 Cyclic motion control for programmable bevel-tip needle 3D steering: a simulation study *2018 IEEE Int. Conf. on Robotics and Biomimetics (ROBIO) (Kuala Lumpur, Malaysia)* (IEEE) pp 444–9
- Cambridge Dictionary 2023 Hypodermic needle (available at: <https://dictionary.cambridge.org/dictionary/english/needle?q=hypodermic+needle>)
- Scali M, Pusch T P, Breedveld P and Dodou D 2017 Ovipositor-inspired steerable needle: design and preliminary experimental evaluation *Bioinspir. Biomim.* **13** 016006
- Suzuki M, Sawa T, Takahashi T and Aoyagi S 2015 Fabrication of microneedle mimicking mosquito proboscis using nanoscale 3D laser lithography system *Int. J. Autom. Technol.* **9** 655–61
- Sahlabadi M, Khodaei S, Jezler K and Hutapea P 2017 Study of bioinspired surgery needle advancing in soft tissues *Proc. of the ASME 2017 Conf. on Smart Materials, Adaptive Structures and Intelligent Systems Volume 1: Development and Characterization of Multifunctional Materials; Mechanics and Behavior of Active Materials; Bioinspired Smart Materials and Systems; Energy Harvesting; Emerging Technologies (Snowbird, Utah, USA)* (American Society of Mechanical Engineers) p V001T06A016
- Zhang X, Chen G, Yu Y, Sun L and Zhao Y 2020 Bioinspired adhesive and antibacterial microneedles for versatile transdermal drug delivery *Research* **2020** 1–9
- Chen Z, He J, Qi J, Zhu Q, Wu W and Lu Y 2020 Long-acting microneedles: a progress report of the state-of-the-art techniques *Drug Discov. Today* **25** 1462–8
- Kim J, Park S, Nam G, Choi Y, Woo S and Yoon S-H 2018 Bioinspired microneedle insertion for deep and precise skin penetration with low force: why the application of mechanophysical stimuli should be considered *J. Mech. Behav. Biomed. Mater.* **78** 480–90
- Roesthuis R 2011 Mechanics of needle-tissue interaction *IEEE Int. Conf. on Intelligent Robots and Systems* pp 2557–63

- [10] Mahvash M and Dupont P E 2010 Mechanics of dynamic needle insertion into a biological material *IEEE Trans. Biomed. Eng.* **57** 934–43
- [11] Makvandi P et al 2022 Bioinspired microneedle patches: biomimetic designs, fabrication and biomedical applications *Matter* **5** 390–429
- [12] Scali M, Kreeft D, Breedveld P and Dodou D 2017 Design and evaluation of a wasp-inspired steerable needle *Proc. SPIE* **10162** 1016207
- [13] Merriam-Webster 2023 Needle (available at: www.merriam-webster.com/dictionary/needle)
- [14] Sahlabadi M and Hutapea P 2018 Novel design of honeybee-inspired needles for percutaneous procedure *Bioinspir. Biomim.* **13** 036013
- [15] Li Y, Zhou W, Liu C, Geng D, Dai J, Xie Y, Chen S, Luo T and Shen Z 2021 Fabrication and characteristic of flexible dry bioelectrodes with microstructures inspired by golden margined century plant leaf *Sensors Actuators A* **321** 112397
- [16] Zhang X, Fu X, Chen G, Wang Y and Zhao Y 2021 Versatile ice microneedles for transdermal delivery of diverse actives *Adv. Sci.* **8** 2101210
- [17] Suzuki M, Sawa T, Takahashi T and Aoyagi S 2015 Ultrafine three-dimensional (3D) laser lithographic fabrication of microneedle and its application to painless insertion and blood sampling inspired by mosquito *2015 IEEE/RSJ Int. Conf. on Intelligent Robots and Systems (IROS) (Hamburg, Germany)* (IEEE) pp 2748–53
- [18] Cai Y, Huang S, Zhang Z, Zhang J, Zhu X, Chen X and Ding X 2022 Bioinspired rotation microneedles for accurate transdermal positioning and ultramiminal-invasive biomarker detection with mechanical robustness *Research* **2022** 1–15
- [19] Wang J Y and Cong Q 2013 Experimental study of the concave bionic drag reduction needles *Appl. Mech. Mater.* **461** 702–6
- [20] Cho W K et al 2012 Microstructured barbs on the North American porcupine quill enable easy tissue penetration and difficult removal *Proc. Natl Acad. Sci.* **109** 21289–94
- [21] Zhang X, Chen G, Cai L, Wang Y, Sun L and Zhao Y 2021 Bioinspired pagoda-like microneedle patches with strong fixation and hemostasis capabilities *Chem. Eng. J.* **414** 128905
- [22] Deng Y, Yang C, Zhu Y, Liu W, Li H, Wang L, Chen W, Wang Z and Wang L 2022 Lamprey-teeth-inspired oriented antibacterial sericin microneedles for infected wound healing improvement *Nano Lett.* **22** 2702–11
- [23] Zhang X, Wang F, Yu Y, Chen G, Shang L, Sun L and Zhao Y 2019 Bio-inspired clamping microneedle arrays from flexible ferrofluid-configured moldings *Sci. Bull.* **64** 1110–7
- [24] Zhang X, Chen G, Sun L, Ye F, Shen X and Zhao Y 2021 Claw-inspired microneedle patches with liquid metal encapsulation for accelerating incisional wound healing *Chem. Eng. J.* **406** 126741
- [25] Guo M, Wang Y, Gao B and He B 2021 Shark tooth-inspired microneedle dressing for intelligent wound management *ACS Nano* **15** 15316–27
- [26] Jeon E Y, Lee J, Kim B J, Joo K I, Kim K H, Lim G and Cha H J 2019 Bio-inspired swellable hydrogel-forming double-layered adhesive microneedle protein patch for regenerative internal/external surgical closure *Biomaterials* **222** 119439
- [27] Yang S Y, O’Cearbhaill E D, Sisk G C, Park K M, Cho W K, Villiger M, Bouma B E, Pomahac B and Karp J M 2013 A bio-inspired swellable microneedle adhesive for mechanical interlocking with tissue *Nat. Commun.* **4** 1702
- [28] Liu S, Chu S, Banis G E, Beardslee L A and Ghodssi R 2020 Biomimetic barbed microneedles for highly robust tissue anchoring *2020 IEEE 33rd Int. Conf. on Micro Electro Mechanical Systems (MEMS) (Vancouver, BC, Canada)* (IEEE) pp 885–8
- [29] Chen Z, Lin Y, Lee W, Ren L, Liu B, Liang L, Wang Z and Jiang L 2018 Additive manufacturing of honeybee-inspired microneedle for easy skin insertion and difficult removal *ACS Appl. Mater. Interfaces* **10** 29338–46
- [30] Izumi H, Suzuki M, Kanzaki T and Aoyagi S 2009 Realistic imitation of mosquito’s proboscis -sharp and jagged needle and their cooperative inserting motion- *TRANSDUCERS 2009 - 2009 Int. Solid-State Sensors, Actuators and Microsystems Conf. (Denver, CO, USA)* (IEEE) pp 2270–3
- [31] Li Q et al 2022 Smart mushroom-inspired printable and lightly detachable (mild) microneedle patterns for effective COVID-19 vaccination and decentralized information storage *ACS Nano* **16** 7512–24
- [32] Aoyagi S, Izumi H and Fukuda M 2008 Biodegradable polymer needle with various tip angles and consideration on insertion mechanism of mosquito’s proboscis *Sensors Actuators A* **143** 20–28
- [33] Chen Z, Ren L, Li J, Yao L, Chen Y, Liu B and Jiang L 2018 Rapid fabrication of microneedles using magnetorheological drawing lithography *Acta Biomater.* **65** 283–91
- [34] Frasson L, Parittotokkaporn T, Davies B L and Rodriguez y Baena F 2008 Early developments of a novel smart actuator inspired by nature *2008 15th Int. Conf. on Mechatronics and Machine Vision in Practice (Auckland, New Zealand)* (IEEE) pp 163–8
- [35] Frasson L, Parittotokkaporn T, Schneider A, Davies B L, Vincent J F V, Huq S E, Degenar P and Rodriguez y Baena F M 2008 Biologically inspired microtexturing: investigation into the surface topography of next-generation neurosurgical probes *2008 30th Annual Int. Conf. of the IEEE Engineering in Medicine and Biology Society (Vancouver, BC)* (IEEE) pp 5611–4
- [36] Schneider A, Frasson L, Parittotokkaporn T, Rodriguez y Baena F M, Davies B L and Ejaz Huq S 2009 Biomimetic microtexturing for neurosurgical probe surfaces to influence tribological characteristics during tissue penetration *Microelectron. Eng.* **86** 1515–7
- [37] Gidde S T R, Acharya S R, Kandel S, Pleshko N and Hutapea P 2022 Assessment of tissue damage from mosquito-inspired surgical needle *Minim. Invasive Ther. Allied Technol.* **31** 1112–21
- [38] Gidde S T R, Islam S, Kim A and Hutapea P 2023 Experimental study of mosquito-inspired needle to minimize insertion force and tissue deformation *Proc. Inst. Mech. Eng. H* **237** 113–23
- [39] Gidde S T R, Ciuciu A, Devaravar N, Doracio R, Kianzad K and Hutapea P 2020 Effect of vibration on insertion force and deflection of bioinspired needle in tissues *Bioinspir. Biomim.* **15** 054001
- [40] Sahlabadi M and Hutapea P 2018 Tissue deformation and insertion force of bee-stinger inspired surgical needles *J. Med. Devices* **12** 034501
- [41] Sahlabadi M, Khodaei S, Jezler K and Hutapea P 2018 Insertion mechanics of bioinspired needles into soft tissues *Minim. Invasive Ther. Allied Technol.* **27** 284–91
- [42] Giovannini M, Ren H, Wang X and Ehmann K 2017 Tissue cutting with microerrated biopsy punches *J. Micro Nano-Manuf.* **5** 041004
- [43] Sravani K G, Desala R K, Chand P, Sathvik K, Rao K S and Lay-Ekuakille A 2022 Design and analysis of bio-inspired micro-needle for drug delivery applications *IEEE Trans. NanoBioscience* **22** 237–44
- [44] Gittard S D, Narayan R J, Ovshnikov A and Chichkov B N 2009 Rapid prototyping of biomimetic structures: fabrication of mosquito-like microneedles by two-photon polymerization *MRS Proc.* **1239** 1239-VV01–11
- [45] Han D, Morde R S, Mariani S, La Mattina A A, Vignali E, Yang C, Barillaro G and Lee H 2020 4D printing of a bioinspired microneedle array with backward-facing barbs for enhanced tissue adhesion *Adv. Funct. Mater.* **30** 1909197
- [46] Hara Y, Yamada M, Tatsukawa C, Takahashi T, Suzuki M and Aoyagi S 2016 Fabrication of stainless steel microneedle with laser-cut sharp tip and its penetration and blood sampling performance *Int. J. Autom. Technol.* **10** 950–7
- [47] Hara Y, Yamada M, Tatsukawa C, Takahashi T, Suzuki M and Aoyagi S 2016 Laser fabrication of jagged-shaped stainless

- steel microneedle imitating mosquito's maxilla *Int. J. Autom. Technol.* **10** 958–64
- [48] Izumi H, Yajima T, Aoyagi S, Tagawa N, Arai Y, Hirata M and Yorifuji S 2008 Combined harpoonlike jagged microneedles imitating mosquito's proboscis and its insertion experiment with vibration *IEEJ Trans. Electr. Electron. Eng.* **3** 425–31
- [49] Izumi H, Suzuki M, Aoyagi S and Kanzaki T 2011 Realistic imitation of mosquito's proboscis: electrochemically etched sharp and jagged needles and their cooperative inserting motion *Sensors Actuators A* **165** 115–23
- [50] Li A D R, Putra K B, Chen L, Montgomery J S and Shih A 2020 Mosquito proboscis-inspired needle insertion to reduce tissue deformation and organ displacement *Sci. Rep.* **10** 12248
- [51] Li F, Huang Z and Xu L 2019 Path planning of 6-DOF venipuncture robot arm based on improved a-star and collision detection algorithms 2019 *IEEE Int. Conf. on Robotics and Biomimetics (ROBIO) (Dali, China)* (IEEE) pp 2971–6
- [52] Li X et al 2021 Limpet tooth-inspired painless microneedles fabricated by magnetic field-assisted 3D printing *Adv. Funct. Mater.* **31** 2003725
- [53] Liu S, Chu S, Beardslee L A and Ghodssi R 2020 Hybrid and passive tissue-anchoring mechanism for ingestible resident devices *J. Microelectromech. Syst.* **29** 706–12
- [54] Lu Y et al 2022 A honeybee stinger-inspired self-interlocking microneedle patch and its application in myocardial infarction treatment *Acta Biomater.* **153** 386–98
- [55] Mizuno Y et al 2021 Fabrication of novel-shaped microneedles to overcome the disadvantages of solid microneedles for the transdermal delivery of insulin *Biomed. Microdevices* **23** 38
- [56] Oka K, Aoyagi S, Arai Y, Isono Y, Hashiguchi G and Fujita H 2002 Fabrication of a micro needle for a trace blood test *Sensors Actuators A* **97-98** 478–85
- [57] Plamadela C et al 2020 Bio-inspired microneedle design for efficient drug/vaccine coating *Biomed. Microdevices* **22** 8
- [58] Suzuki M, Takahashi T and Aoyagi S 2018 3D laser lithographic fabrication of hollow microneedle mimicking mosquitos and its characterisation *Int. J. Nanotechnol.* **15** 157
- [59] Suzuki M, Sawa T, Terada Y, Takahashi T and Aoyagi S 2015 Fabrication of microneedles precisely imitating mosquito's proboscis by nanoscale tree dimensional laser lithography and its characterization 2015 *Transducers - 2015 18th Int. Conf. on Solid-State Sensors, Actuators and Microsystems (Transducer) (Anchorage, AK, USA)* (IEEE) pp 121–4
- [60] Tran L-G, Nguyen T-Q and Park W-T 2019 Bio-inspired barbed microneedle for skin adhesion with interlocking mechanics 2019 *IEEE 32nd Int. Conf. on Micro Electro Mechanical Systems (MEMS) (Seoul, Korea (South))* (IEEE) pp 547–50
- [61] Tsuchiya K, Isobata K, Sato M, Uetsuji Y, Nakamachi E, Kajiwara K and Kimura M 2007 Design of painless microneedle for blood extraction system *Proc. SPIE* **6799** 67990Q
- [62] Velivela P T, Letov N, Liu Y and Fiona Zhao Y 2021 Application of domain integrated design methodology for bio-inspired design - a case study of suture pin design *Proc. Des. Soc.* **1** 487–96
- [63] Wang J, Chen Y, Ren L, Li Y and Zhou C 2016 Bionic technology research study based on the non-smooth surface morphology of the mosquito mouthparts 2016 *6th Int. Conf. on Mechatronics, Computer and Education Informatization (MCEI 2016) (Shenyang, China)* (<https://doi.org/10.2991/mcei-16.2016.72>)
- [64] Fu X, Zhang X, Huang D, Mao L, Qiu Y and Zhao Y 2022 Bioinspired adhesive microneedle patch with gemcitabine encapsulation for pancreatic cancer treatment *Chem. Eng. J.* **431** 133362
- [65] Joymungul K, Mitros Z, da Cruz L, Bergeles C and Sadati S 2021 *Gripe-needle: a sticky suction cup gripper equipped needle for targeted therapeutics delivery* *Front. Robot. AI* **8** 752290
- [66] Suzuki M, Motooka F, Takahashi T and Aoyagi S 2020 Development of microneedle puncture device that prevents buckling of needle by delivery operation *J. Robot. Mechatronics* **32** 382–9
- [67] Scali M, Breedveld P and Dodou D 2019 Experimental evaluation of a self-propelling bio-inspired needle in single- and multi-layered phantoms *Sci. Rep.* **9** 19988
- [68] O'Ceirbhail E D, Lulicht B, Mitchell N, Yu L, Valic M, Masiakos P and Karp J M 2019 A radial clutch needle for facile and safe tissue compartment access *Med. Devices Sens.* **2** e10049
- [69] Bloemberg J, Trauzettel F, Coolen B, Dodou D and Breedveld P 2022 Design and evaluation of an MRI-ready, self-propelled needle for prostate interventions *PLoS One* **17** e0274063
- [70] Frasson L, Ferroni F, Ko S Y, Dogangil G and Rodriguez y Baena F 2012 Experimental evaluation of a novel steerable probe with a programmable bevel tip inspired by nature *J. Robot. Surg.* **6** 189–97
- [71] Ko S Y, Frasson L and Rodriguez y Baena F 2011 Closed-loop planar motion control of a steerable probe with a "programmable bevel" inspired by nature *IEEE Trans. Robot.* **27** 970–83
- [72] Ko S Y and Rodriguez y Baena F 2013 Toward a miniaturized needle steering system with path planning for obstacle avoidance *IEEE Trans. Biomed. Eng.* **60** 910–7
- [73] Sprang T, Breedveld P and Dodou D 2016 Wasp-inspired needle insertion with low net push force *Biomimetic and Biohybrid Systems (Lecture Notes in Computer Science)* vol 9793, ed N F Lepora, A Mura, M Mangan, P F M J Verschure, M Desmulliez and T J Prescott (Cham: Springer) pp 307–18
- [74] Burrows C, Secoli R and Rodriguez y Baena F 2013 Experimental characterisation of a biologically inspired 3D steering needle 2013 *13th Int. Conf. on Control, Automation and Systems (ICCAS 2013) (Gwangju, Korea (South))* pp 1252–7
- [75] Burrows C, Liu F and Rodriguez y Baena F 2015 Smooth on-line path planning for needle steering with non-linear constraints 2015 *IEEE/RSJ Int. Conf. on Intelligent Robots and Systems (IROS) (Hamburg, Germany)* (IEEE) pp 2653–8
- [76] Ko S Y and Rodriguez y Baena F 2012 Trajectory following for a flexible probe with state/input constraints: an approach based on model predictive control *Robot. Auton. Syst.* **60** 509–21
- [77] Leibinger A, Oldfield M J and Rodriguez y Baena F 2016 Minimally disruptive needle insertion: a biologically inspired solution *Interface Focus* **6** 20150107
- [78] Matheson E and Rodriguez y Baena F 2020 Biologically inspired surgical needle steering: technology and application of the programmable bevel-tip needle *Biomimetics* **5** 68
- [79] Matheson E, Secoli R, Burrows C, Leibinger A and Rodriguez y Baena F 2019 Cyclic motion control for programmable bevel-tip needles to reduce tissue deformation *J. Med. Robot. Res.* **04** 1842001
- [80] Oldfield M J, Burrows C, Kerl J, Frasson L, Parittotokkaporn T, Beyrau F and Rodriguez y Baena F 2014 Highly resolved strain imaging during needle insertion: results with a novel biologically inspired device *J. Mech. Behav. Biomed. Mater.* **30** 50–60
- [81] Oldfield M J, Leibinger A, Seah T E T and Rodriguez y Baena F 2015 Method to reduce target motion through needle-tissue interactions *Ann. Biomed. Eng.* **43** 2794–803
- [82] Secoli R, Rodriguez F and Baena 2018 Experimental validation of curvature tracking with a programmable bevel-tip steerable needle 2018 *Int. Symp. on Medical Robotics (ISMR) (Atlanta, GA, USA)* (IEEE) pp 1–6
- [83] Virdyawan V, Oldfield M and Rodriguez y Baena F 2018 Laser doppler sensing for blood vessel detection with a biologically inspired steerable needle *Bioinspir. Biomim.* **13** 026009
- [84] Virdyawan V and Rodriguez Y Baena F 2018 Vessel pose estimation for obstacle avoidance in needle steering surgery

- using multiple forward looking sensors *2018 IEEE/RSJ Int. Conf. on Intelligent Robots and Systems (IROS) (Madrid)* (IEEE) pp 3845–52
- [85] Culmone C, Smit G and Breedveld P 2019 Additive manufacturing of medical instruments: a state-of-the-art review *Addit. Manuf.* **27** 461–73
- [86] Rahamim V and Azagury A 2021 Bioengineered biomimetic and bioinspired noninvasive drug delivery systems *Adv. Funct. Mater.* **31** 2102033
- [87] Yoshida Y and Takei T 2009 Fabrication of a microneedle using human hair *Jpn. J. Appl. Phys.* **48** 098007
- [88] Olatunji O, Igwe C C, Ahmed A S, Alhassan D O A, Asieba G O and Diganta B D 2014 Microneedles from fish scale biopolymer *J. Appl. Polym. Sci.* **131** 40377
- [89] Gao Y, Zhang W, Fang Cheng Y, Cao Y, Xu Z, Xu Li Q, Kang Y and Xue P 2021 Intradermal administration of green synthesized nanosilver (NS) through film-coated PEGDA microneedles for potential antibacterial applications *Biomater. Sci.* **9** 2244–54
- [90] Zhang W, Zhang Y and Liu Y 2021 Design and control of a bionic needle puncture robot *Int. J. Med. Robot. Comput. Assist. Surg.* **17** e2200
- [91] Burrows C, Liu F, Leibinger A, Secoli R and Rodriguez y Baena F 2017 Multi-target planar needle steering with a bio-inspired needle design *Advances in Italian Mechanism Science (Mechanisms and Machine Science)* vol 47, ed G Boschetti and A Gasparetto (Cham: Springer) pp 51–60
- [92] Frasson L, Ko S Y, Turner A, Parittotokkaporn T, Vincent J F and Rodriguez y Baena F 2010 Sting: a soft-tissue intervention and neurosurgical guide to access deep brain lesions through curved trajectories *Proc. Inst. Mech. Eng. H* **224** 775–88
- [93] Li H, Huy Nguyen V and Zhang H 2019 Nature inspired conceptual design of a micro neural probe for deep brain stimulation *Sustainable Design and Manufacturing 2018 (Smart Innovation, Systems and Technologies)* vol 130, ed D Dao, R J Howlett, R Setchi and L Vlacic (Cham: Springer) pp 31–40
- [94] Chen D, Li J, Zhao J, Guo J, Zhang S, Sherazi T A, Khan A and Li S 2018 Bioinspired superhydrophilic-hydrophobic integrated surface with conical pattern-shape for self-driven fog collection *J. Colloid Interface Sci.* **530** 274–81
- [95] Tsuchiya K, Nakanishi N and Nakamachi E 2004 Development of blood extraction system for health monitoring system *Proc. SPIE* **5275** 257–65